

# Control of continuous-mode single-photon states: a review

Guofeng Zhang\*

July 14, 2021

## Abstract

In this survey, we first introduce quantum fields and open quantum systems, then we present continuous-mode single-photon states and discuss discrete measurements of a single-photon field. After that, we introduce linear quantum systems and show how a linear quantum system responds to a single-photon input. Then we investigate how a coherent feedback network can be used to manipulate the temporal pulse shape of a single-photon state. Afterwards, we present single-photon filter and master equations. Finally, we discuss the generation of Schrödinger cat states by means of photon addition and subtraction.

**Keywords:** Quantum control, continuous-mode single photon states, coherent feedback, filtering, master equations, Schrödinger cat states.

## Contents

<b>1</b>	<b>Introduction</b>	<b>2</b>
<b>2</b>	<b>Open quantum systems</b>	<b>3</b>
2.1	Field . . . . .	4
2.2	System . . . . .	6
<b>3</b>	<b>Continuous-mode single-photon states</b>	<b>9</b>
3.1	Discrete measurement of a continuous-mode single-photon state . . . . .	14
<b>4</b>	<b>Linear systems' response to single-photon states</b>	<b>16</b>
<b>5</b>	<b>Single-photon pulse shaping via coherent feedback</b>	<b>21</b>
<b>6</b>	<b>Single-photon filter and master equation</b>	<b>22</b>

---

\*Department of Applied Mathematics, The Hong Kong Polytechnic University, Hong Kong. Email: guofeng.zhang@polyu.edu.hk.

## 1 Introduction

A light field is said to be in an  $\ell$ -photon state if it contains *exactly*  $\ell$  photons. When  $\ell = 1$ , it is in a single-photon state. An optical or microwave photon, as an electromagnetic field, has discrete degrees of freedom like polarization; it also has continuous degrees of freedom, for example a photon can be viewed as a wavepacket with a continuous spectral or spatial envelope. In this review, we are interested in continuous-mode single-photon states. Due to their highly genuine quantum nature, single- and few-photon states hold promising applications in quantum communication, quantum computation, quantum metrology and quantum simulations. Recently, there has been a rapidly growing interest in the generation, communication, storage, and manipulation (e.g., pulse shaping) of few-photon states. Thus, a new burgeoning and important problem in the field of quantum engineering is: How to analyze and design quantum dynamical systems driven by few-photon states so as to achieve desirable control performance; for example, producing a single photon with pre-specified pulse shape? In this review, we investigate single-photon states from a control-theoretic perspective. For physical implementation of single photon generation, detection and storing, please refer to the physics literature [1–19] and references therein.

Interaction between a photon (flying qubit information carrier) and a two-level emitter (stationary qubit information carrier) is fundamental to quantum information processing and quantum physics. Efficient interaction is achieved when the incident photon has a well-defined temporal or frequency modal structure which matches that of the stationary qubit. For example, for atomic excitation by a single photon, it is well-known [20–22] that on resonance the optimal excitation by a single photon of a rising exponential pulse shape is achieved when  $\gamma = \kappa$ , where  $\gamma$  is the full width at half maximum (FWHM) of the photon wave packet and  $\kappa$  is the decay rate of the two-level atom. On the other hand, if the incident photon is of a Gaussian pulse shape, the optimal ratio is 0.8 which is achieved when  $\Omega = 1.46\kappa$ , where  $\Omega$  is the photon frequency bandwidth [20, 21, 23–25]. When a two-level atom is driven by two co-propagating photons of Gaussian pulse shape, numerical simulations in [26] show that the maximum excitation probability is around 0.88 attained at  $\Omega = 2 * 1.46\kappa$ . Moreover, when a two-level atom is driven by two counter-propagating identical photons, it is shown in [27, 28] that the maximum excitation probability is attained at  $\gamma = 5\kappa$  for rising exponential pulse shapes, and  $\Omega = 2 * 1.46\kappa$  for the Gaussian pulse shapes.

The rest of this article is organized as follows. Open quantum systems are briefly introduced in Section 2. Continuous-mode single-photon states are presented in Section 3. The response of a quantum linear system to a single-photon input is discussed in Section 4. In Section 5 it

is shown how to use a linear coherent feedback network to shape the temporal pulse of a single photon. Single-photon filters and master equations are presented in Section 6. Schrödinger cat states generation is discussed in Section 7. Two possible future research problems are proposed in Section 8.

*Notation.* The reduced Planck constant  $\hbar$  is set to 1.  $|0\rangle$  stands for the vacuum (namely no photon) state of a free-propagating light field. Given a column vector of operators or complex numbers  $X = [x_1, \dots, x_n]^\top$ , the Hilbert space adjoint operator or complex conjugate of  $X$  is denoted by  $X^\# = [x_1^*, \dots, x_n^*]^\top$ . Let  $X^\dagger = (X^\#)^\top$  and  $\check{X} = [X^\top, X^\dagger]^\top$ . The commutator between operators  $A$  and  $B$  is defined to be  $[A, B] \triangleq AB - BA$ . Given operators  $L, H, X, \rho$ , define two superoperators

$$\begin{aligned} \text{Lindbladian : } \mathcal{L}_G X &\triangleq -i[X, H] + \mathcal{D}_L X, \\ \text{Liouvillian : } \mathcal{L}_G^* \rho &\triangleq -i[H, \rho] + \mathcal{D}_L^* \rho, \end{aligned}$$

where  $\mathcal{D}_L X = L^\dagger X L - \frac{1}{2}(L^\dagger L X + X L^\dagger L)$ , and  $\mathcal{D}_L^* \rho = L \rho L^\dagger - \frac{1}{2}(L^\dagger L \rho + \rho L^\dagger L)$ .  $\omega_c$  is the system frequency such as the resonance frequency of a cavity mode (which is a quantum harmonic oscillator) or the transition frequency of a two-level system.  $\omega_o$  is the carrier frequency of an external field.  $\omega_d = \omega_c - \omega_o$  is the frequency detuning.  $\delta_{jk}$  is the Kronecker delta function and  $\delta(t - r)$  is the Dirac delta function. The Fourier transform of a time-domain function  $\xi \in L_2(\mathbb{R}, \mathbb{C})$  generates

$$\xi[i\nu] = \frac{1}{\sqrt{2\pi}} \int_{-\infty}^{\infty} e^{i\nu t} \xi(t) dt$$

in the frequency domain, whose inverse Fourier transform is

$$\xi(t) = \frac{1}{\sqrt{2\pi}} \int_{-\infty}^{\infty} e^{-i\nu t} \xi[i\nu] d\nu. \quad (1.1)$$

## 2 Open quantum systems

In this section, we briefly introduce open quantum systems, as shown in Fig. 1. Interested readers may refer to references [29–38] for more detailed discussions.

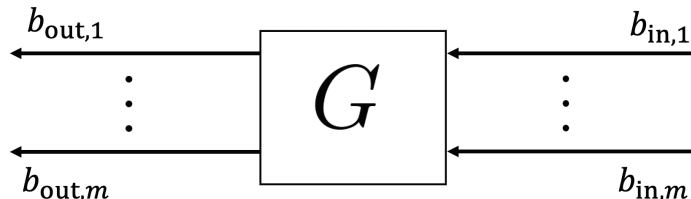


Figure 1: A quantum system  $G$  with  $m$  input fields and  $m$  output fields

## 2.1 Field

In quantum physics, a free propagating Boson field is mathematically modeled by a continuum of quantum harmonic oscillators, represented by their annihilation operators  $b_\omega$  and creation operators  $b_\omega^*$  (the Hilbert space adjoints of  $b_\omega$ ). Here,  $\omega$  stands for frequencies. These field operators satisfy singular commutation relations

$$[b_\omega, b_{\omega'}] = [b_\omega^*, b_{\omega'}^*] = 0, \quad [b_\omega, b_{\omega'}^*] = \delta(\omega - \omega'). \quad (2.1)$$

Physically,  $b_\omega$  annihilates a photon in the field. Hence, if there is no photon in the field, in other words, the field is in the vacuum state  $|0\rangle$ , then  $b_\omega |0\rangle = 0$ . The Hamiltonian of the field is

$$H_B = \int_0^\infty d\omega \omega b_\omega^\dagger b_\omega. \quad (2.2)$$

By (2.1), in the Heisenberg picture, the free evolution of  $b_\omega$  is governed by

$$b_\omega(t) = e^{iH_B t} b_\omega e^{-iH_B t} = e^{-i\omega t} b_\omega. \quad (2.3)$$

Hence,

$$H_B(t) = \int_0^\infty d\omega \omega b_\omega^\dagger(t) b_\omega(t) = H_B, \quad (2.4)$$

i.e., the Hamiltonian of a free-evolution field is independent of time.

For open quantum systems, we are interested in the interaction between the field and the system of interest, starting from an initial time. In this paper, we use  $t_0$  to denote the initial time. After the initial time, the field does not evolve on its own due to its interaction with the system. As a result, (2.4) does not hold any longer. Instead, the field will carry system's information. It is because of this that the system can be read when the field is measured.

**Remark 2.1.** A quantum system has a characteristic frequency, e.g., the atomic transition frequency between energy levels of an atom, the resonant frequency of a quantum cavity resonator, or the Rabi frequency of a continuous-wave (cw) driving laser. When the system interacts with an input field (often called incident field in quantum optics), it is a standard assumption that only the field modes whose frequencies are near the characteristic frequency of the system contribute to the interaction with the system, while the influence of those modes whose frequencies are far away from the characteristic frequency of the system is negligible. In other words, it is often the case that the *effective* field is within a narrow sideband centered at this characteristic frequency. Under this assumption (narrow band approximation), the range of integral of (2.2) can be extended from  $-\infty$  to  $\infty$ . More discussions can be found in, e.g., [39, 40].

In the input-output formalism of open quantum systems, the input field in the time domain is defined as (see e.g. [39, (4)], [40, (2.14)], [41, Sec. III])

$$b_{\text{in}}(t) \triangleq \frac{1}{\sqrt{2\pi}} \int_{-\infty}^{\infty} d\omega e^{-i\omega(t-t_0)} b_\omega(t_0), \quad t \geq t_0, \quad (2.5)$$

where  $b_\omega(t_0)$  denotes the quantum harmonic oscillator  $b_\omega$  at the initial time  $t_0$ . It can be seen from (2.3) and (2.5) that  $b_{\text{in}}(t)$  is a continuum of quantum harmonic oscillators  $b_\omega$  for all frequencies.  $b_{\text{in}}^*(t)$ , the adjoint of  $b_{\text{in}}(t)$ , is obtained by conjugating both sides of (2.5),

$$b_{\text{in}}^*(t) = \frac{1}{\sqrt{2\pi}} \int_{-\infty}^{\infty} e^{i\omega(t-t_0)} b_\omega^*(t_0) d\omega, \quad t \geq t_0.$$

By (2.1), we have the singular commutation relations for  $b_{\text{in}}(t)$  and  $b_{\text{in}}^*(t)$  in the time domain,

$$[b_{\text{in}}(t_1), b_{\text{in}}(t_2)] = [b_{\text{in}}^*(t_1), b_{\text{in}}^*(t_2)] = 0, \quad [b_{\text{in}}(t_1), b_{\text{in}}^*(t_2)] = \delta(t_1 - t_2), \quad t_1, t_2 \geq t_0. \quad (2.6)$$

For the input field  $b_{\text{in}}(t)$  in the time domain defined in (2.5), we define its Fourier transform as

$$b_{\text{in}}[i\omega] \triangleq \frac{1}{\sqrt{2\pi}} \int_{t_0}^{\infty} dt e^{i\omega t} b_{\text{in}}(t), \quad \omega \in \mathbb{R}. \quad (2.7)$$

The adjoint  $b_{\text{in}}^*[i\omega]$  of  $b_{\text{in}}[i\omega]$  is obtained by conjugating both sides of (2.7); specifically,

$$b_{\text{in}}^*[i\omega] = \frac{1}{\sqrt{2\pi}} \int_{t_0}^{\infty} dt e^{-i\omega t} b_{\text{in}}^*(t), \quad \omega \in \mathbb{R}.$$

Noticing the identity

$$\lim_{t_0 \rightarrow -\infty} \frac{1}{2\pi} \int_{t_0}^{\infty} dt e^{i\omega t} = \delta(\omega),$$

it can be readily shown that

$$\lim_{t_0 \rightarrow -\infty} [b_{\text{in}}[i\omega], b_{\text{in}}^*[i\omega']] = \delta(\omega - \omega'), \quad \omega, \omega' \in \mathbb{R}. \quad (2.8)$$

**Remark 2.2.** For any fixed  $t_0$ , applying the inverse Fourier transform to (2.5) yields

$$b_\omega(t_0) e^{i\omega t_0} = \frac{1}{\sqrt{2\pi}} \int_{-\infty}^{\infty} e^{i\omega t} b_{\text{in}}(t) dt, \quad t \geq t_0.$$

This, together with (2.3), gives

$$b_\omega = \frac{1}{\sqrt{2\pi}} \int_{-\infty}^{\infty} e^{i\omega t} b_{\text{in}}(t) dt, \quad t \geq t_0. \quad (2.9)$$

In the limit  $t_0 \rightarrow -\infty$ , (2.7) and (2.9) yield

$$b_{\text{in}}[i\omega] = b_\omega, \quad (2.10)$$

which confirms consistency between (2.1) and (2.8).

**Remark 2.3.** In the definition of  $b_{\text{in}}(t)$  in (2.5), if we **implicitly** assume that  $b_{\text{in}}(t) \equiv 0$  for  $t < t_0$ , then (2.7) becomes

$$b_{\text{in}}[i\omega] = \frac{1}{\sqrt{2\pi}} \int_{-\infty}^{\infty} dt e^{i\omega t} b_{\text{in}}(t), \quad \omega \in \mathbb{R}, \quad (2.11)$$

which is the same as (2.9). As a result, (2.10) holds without taking the limit  $t_0 \rightarrow -\infty$ . Indeed, by (2.3) and (2.5), we have

$$b_{\text{in}}(t) = \frac{1}{\sqrt{2\pi}} \int_{-\infty}^{\infty} e^{-i\omega t} b_{\omega} d\omega, \quad t \geq t_0. \quad (2.12)$$

Thus, under the assumption that  $b_{\text{in}}(t) \equiv 0$  for  $t < t_0$ , Fourier transforming (2.12) yields (2.10), i.e.,

$$b_{\omega} = \frac{1}{\sqrt{2\pi}} \int_{-\infty}^{\infty} dt e^{i\omega t} b_{\text{in}}(t) = b_{\text{in}}[i\omega], \quad (2.13)$$

where (2.11) has been used. In view of this, it appears meaningful to interpret the variable “ $t$ ” in (2.5) as the real time under the assumption that  $b_{\text{in}}(t) \equiv 0$  for  $t < t_0$  where  $t_0$  is the time when the system and the field start their interaction. This is fine as we are interested in the dynamics of open quantum systems, instead of free evolution of the system or the field itself. (This interpretation is different from that in [42, Sec. 2.2].) In the study of stochastic Schrödinger equations it is always assumed that  $t_0 = 0$  or some finite value. On the other hand, in the study of photon scattering off a standing emitter, it is often assumed that  $t_0 = -\infty$ , i.e. the interaction starts in the remote past. Under the treatment proposed above, the specific value of the initial time  $t_0$  is not important.

We end this subsection as a final remark.

**Remark 2.4.** *In this review, we often omit the subscript “in” for the input fields. Thus  $b(t)$  is the input field in the time domain while  $b[i\omega]$  is the input field in the frequency domain. Clearly,  $b[i\omega]$  and  $b_{\omega}$  are different objects. However, as shown in (2.13), they can be the same under some condition.*

## 2.2 System

The open Markovian quantum system  $G$ , as shown in Fig. 1, can be described in the so-called  $(S, L, H)$  formalism [32, 33, 35, 43]. In this formalism,  $S, L, H$  are operators on the Hilbert space for the system  $G$ . Specifically,  $S$  is a scattering operator that satisfies  $S^{\dagger}S = SS^{\dagger} = I$  (the identity operator). For example,  $S$  can be a phase shifter or beamsplitter,  $L = [L_1, \dots, L_m]^{\top}$  describes how the system  $G$  interacts with its surrounding environment, and the self-adjoint operator  $H$  denotes the inherent system Hamiltonian of  $G$ . The quantum system  $G$  is driven by  $m$  input fields. Denote the annihilation operator of the  $j$ -th Boson input field by  $b_j(t)$  and the creation operator, the adjoint operator of  $b_j(t)$ , by  $b_j^*(t)$ ,  $j = 1, \dots, m$ . Then similar to (2.6), the fields satisfy the following singular commutation relations:

$$[b_j(t), b_k^*(r)] = \delta_{jk} \delta(t - r), \quad j, k = 1, \dots, m, \quad \text{and } t, r \geq t_0. \quad (2.14)$$

Denote a column of vectors  $b(t) = [b_1(t), \dots, b_m(t)]^\top$ . The integrated input annihilation, creation, and gauge processes (counting processes) are given by

$$B(t) = \int_{t_0}^t b(s)ds, \quad B^\#(t) = \int_{t_0}^t b^\#(s)ds, \quad \Lambda(t) = \int_{t_0}^t b^\#(s)b^\top(s)ds, \quad (2.15)$$

respectively. In this paper, the input fields are assumed to be canonical fields which include the vacuum, coherent, single- and multi-photon fields but not the thermal fields. Then these quantum stochastic processes satisfy

$$\begin{aligned} dB_j(t)dB_k^*(t) &= \delta_{jk}dt, & dB_j(t)d\Lambda_{kl}(t) &= \delta_{jk}dB_l(t), \\ d\Lambda_{jk}(t)dB_l^*(t) &= \delta_{kl}dB_j^*(t), & d\Lambda_{jk}(t)d\Lambda_{lm}(t) &= \delta_{kl}d\Lambda_{jm}(t). \end{aligned}$$

According to quantum mechanics, the whole system in Fig. 1 evolves in a unitary manner. Specifically, there is a unitary operator  $U(t)$  on the tensor product System  $\otimes$  Field Hilbert space that governs the temporal evolution of this quantum system. It turns out that the unitary operator  $U(t)$  is the solution to the Itô quantum stochastic differential equation (QSDE)

$$dU(t) = \left\{ - \left( iH + \frac{1}{2}L^\dagger L \right) dt + LdB^\dagger(t) - L^\dagger SdB(t) + \text{Tr}[S - I]d\Lambda(t) \right\} U(t) \quad (2.16)$$

with the initial condition  $U(t_0) = I$ . In particular, if  $L = 0$  and  $S = I$ , then (2.16) reduces to

$$i\dot{U} = HU,$$

which is the Schrödinger equation for an isolated quantum system with Hamiltonian  $H$ .

Using the unitary operator  $U(t)$  in (2.16), the dynamical evolution of system operators and the environment can be obtained in the Heisenberg picture. Indeed, the time evolution of the system operator  $X$ , denoted by

$$j_t(X) \equiv X(t) = U^\dagger(t)(X \otimes I_{\text{field}})U(t), \quad (2.17)$$

follows the Itô QSDE

$$\begin{aligned} dj_t(X) &= j_t(\mathcal{L}_G X)dt + dB^\dagger(t)j_t(S^\dagger[X, L]) + j_t([L^\dagger, X]S)dB(t) \\ &\quad + \text{Tr}[j_t(S^\dagger X S - X)d\Lambda(t)]. \end{aligned}$$

On the other hand, the dynamical evolution of the output field is given by

$$\begin{aligned} dB_{\text{out}}(t) &= L(t)dt + S(t)dB(t), \\ d\Lambda_{\text{out}}(t) &= L^\#(t)L^\top(t)dt + S^\#(t)dB^\#(t)L^\top(t) \\ &\quad + L^\#(t)dB^\top(t)S^\top(t) + S^\#(t)d\Lambda(t)S^\top(t), \end{aligned}$$

where

$$\begin{aligned} B_{\text{out}}(t) &= U^\dagger(t)(I_{\text{system}} \otimes B(t))U(t), \\ \Lambda_{\text{out}}(t) &= U^\dagger(t)(I_{\text{system}} \otimes \Lambda(t))U(t) \end{aligned}$$

are the integrated output annihilation operator and gauge processes, respectively.

**Example 2.1** (Optical cavity). Let  $G$  be an optical cavity. Here we consider the simplest case: the cavity has a single intracavity mode (a quantum harmonic oscillator represented by its annihilation operator  $a$ ) which interacts with an external light field represented by its annihilation operator  $b(t)$ . Because  $a$  is a cavity mode, it and its adjoint operator  $a^*$  satisfy the canonical commutation relation  $[a, a^*]=1$ , in contrast to the singular commutation relation (2.14) for free propagating fields. As introduced in the *Notation* part, let  $\omega_d$  be the detuned frequency between the resonance frequency of the internal mode  $a$  and the central frequency of the external light field  $b(t)$ . Let  $\kappa$  be the half linewidth of the cavity. In the  $(S, L, H)$  formalism, we have  $S = I$ ,  $L = \sqrt{\kappa}a$ , and  $H = \omega_d a^* a$ . Then, the dynamics of this *linear* system can be described in the input-output form

$$\begin{aligned} da(t) &= -(i\omega_d + \frac{\kappa}{2})a(t)dt - \sqrt{\kappa}dB(t), \\ dB_{\text{out}}(t) &= \sqrt{\kappa}a(t)dt + dB(t). \end{aligned} \tag{2.18}$$

Applying the Laplace transform to (2.18) and omitting the influence of the initial state  $a(t_0)$  yield

$$a[i\omega] = -\frac{\sqrt{\kappa}}{i(\omega + \omega_d) + \frac{\kappa}{2}}b[i\omega] = -T[i\omega]b[i\omega],$$

where

$$T[i\omega] \triangleq \frac{\sqrt{\kappa}}{i(\omega + \omega_d) + \frac{\kappa}{2}} \tag{2.19}$$

is called the *amplitude transmission function* in optics literature; see e.g., [44].  $T[i\omega]$  gives the relation between the intra-cavity mode and the input mode and is in the form of a Lorentzian lineshape function; see (3.6). Finally, the value  $T[0] = \frac{\sqrt{\kappa}}{i\omega_d + \frac{\kappa}{2}}$  in the neighborhood of the resonance of the cavity is commonly used in optics.

**Example 2.2** (Two-level system). A two-level system residing in a chiral nanophotonic waveguide can be parametrized by the triple  $S = 1$ ,  $L = \sqrt{\kappa}\sigma_-$ , and  $H = \frac{\omega_d}{2}\sigma_z$ . The two-level system has two energy states: the ground state  $|g\rangle$  and excited state  $|e\rangle$ .  $\sigma_- = |g\rangle\langle e|$  and  $\sigma_+ = |e\rangle\langle g|$  are the lowering and raising operator respectively. We have  $\sigma_-|g\rangle = 0$  and  $\sigma_+|e\rangle = 0$ .  $\sigma_z = |e\rangle\langle e| - |g\rangle\langle g|$  is the Pauli Z operator. The scalar  $\omega_d$  is the detuning frequency between the transition frequency (between  $|g\rangle$  and  $|e\rangle$ ) of the two-level system and the



central frequency of the external light field, and  $\kappa$  is the decay rate of the two-level system. The dynamics of the system are described by

$$\begin{aligned} d\sigma_-(t) &= -(i\omega_d + \frac{\kappa}{2})\sigma_-(t)dt + \sqrt{\kappa}\sigma_z(t)dB(t), \\ dB_{\text{out}}(t) &= \sqrt{\kappa}\sigma_-(t)dt + dB(t). \end{aligned}$$

It should be noted that this system is *bilinear* due to the presence of  $\sigma_z(t)dB(t)$ , in contrast to the linear resonator in Example 2.1. However, if the two-level atom is initially in the ground state  $|g\rangle$  and the field is in the vacuum state  $|0\rangle$ , as  $\sigma_z(t)|g0\rangle = -|g0\rangle$  (see e.g., [22, Lemma 3]), we have

$$\begin{aligned} d\sigma_-(t)|g0\rangle &= -(i\omega_d + \frac{\kappa}{2})\sigma_-(t)dt|g0\rangle - \sqrt{\kappa}dB(t)|g0\rangle, \\ dB_{\text{out}}(t)|g0\rangle &= \sqrt{\kappa}\sigma_-(t)|g0\rangle dt + dB(t)|g0\rangle, \end{aligned}$$

which is in the form of *linear* dynamics. Finally, rotations

$$\sigma_-(t) \rightarrow e^{i\omega_d t}\sigma_-(t), \quad B(t) \rightarrow e^{i\omega_d t}B(t), \quad B_{\text{out}}(t) \rightarrow e^{i\omega_d t}B_{\text{out}}(t)$$

put the above system into the following form

$$\begin{aligned} d\sigma_-(t)|g0\rangle &= -\frac{\kappa}{2}\sigma_-(t)dt|g0\rangle - \sqrt{\kappa}dB(t)|g0\rangle, \\ dB_{\text{out}}(t)|g0\rangle &= \sqrt{\kappa}\sigma_-(t)|g0\rangle dt + dB(t)|g0\rangle. \end{aligned}$$

**Remark 2.5.** In this section, the dynamics of a quantum system are given directly in terms of the system operators  $S, L, H$ . This is unlike the traditional way where the starting point is a total Hamiltonian for the joint system-field system, see, e.g, [39]. Nevertheless, the  $(S, L, H)$  formalism originates from and is a simplified version of the traditional approach [32]. An illustrative example can be found in [26, Example 1].

### 3 Continuous-mode single-photon states

In this section, we introduce single-photon states of a free propagating light field.

Denote  $|1_t\rangle = b^*(t)|0\rangle$ . By (2.14) and  $b(t)|0\rangle = 0$ , we have  $\langle 1_t|1_\tau\rangle = \delta(t - \tau)$ . A continuous-mode single-photon state of a light field having the temporal pulse shape  $\xi(t) \in L_2(\mathbb{R}, \mathbb{C})$  can be viewed as a superposition of the continuum of  $|1_t\rangle$ ; in other words,

$$|1_\xi\rangle \equiv \mathbf{B}^*(\xi)|0\rangle \triangleq \int_{-\infty}^{\infty} \xi(t)|1_t\rangle dt. \quad (3.1)$$

Assume the  $L_2$  norm  $\|\xi\| \triangleq \sqrt{\int_{-\infty}^{\infty} |\xi(t)|^2 dt} = 1$ . (It is assumed that  $\xi(t) \equiv 0$  for  $t < t_0$  (the initial time) as we focus on the interaction between a system and a field.) Then  $\langle 1_\xi|1_\xi\rangle = 1$ .

Hence, the probability of finding the photon in the time interval  $[t, t + dt)$  is  $|\xi(t)|^2 dt$ . In the frequency domain, we use  $|1_\omega\rangle \triangleq b^*[i\omega]|0\rangle$ . In the frequency domain (3.1) becomes

$$|1_\xi\rangle = \int_{-\infty}^{\infty} \xi[i\omega] |1_\omega\rangle d\omega. \quad (3.2)$$

**Remark 3.1.** If we do not restrict  $\xi$  to be in  $L_2(\mathbb{R}, \mathbb{C})$ , for example, let  $\xi[i\omega] = \delta(\omega - \omega_0)$  for some real  $\omega_0$ ; in other words, we have a monochromatic light field with frequency  $\omega_0$ . Then from (3.2) we get

$$|1_\xi\rangle = b^*[i\omega_0]|0\rangle = |1_{\omega_0}\rangle.$$

Moreover, by (1.1) we get the temporal wave packet  $\xi(t) = \frac{1}{\sqrt{2\pi}} e^{i\omega_0 t}$  whose modulus is  $|\xi(t)| \equiv \frac{1}{\sqrt{2\pi}}$  for all  $t \in \mathbb{R}$ .

If a field is restricted to be in the interval  $[t_0, t]$ , (3.1) becomes

$$|1_\xi\rangle = \int_{t_0}^t \xi(r) |1_r\rangle dr.$$

Similarly, an  $\ell$ -photon state of a field over the interval  $[t_0, t]$  can be defined as

$$|\ell_\psi\rangle = \int_{t_0}^t \cdots \int_{t_0}^t \psi(\tau_1, \dots, \tau_\ell) |1_{\tau_1}\rangle \cdots |1_{\tau_\ell}\rangle d\tau_1 \cdots d\tau_\ell. \quad (3.3)$$

In other words, by means of a continuum of basis vectors  $\{|0\rangle, |1_{\tau_1}\rangle, \dots, |1_{\tau_\ell}\rangle : \tau_1, \dots, \tau_\ell \in [t_0, t]\}$ , any  $\ell$ -photon state can be expressed in the way given in (3.3). As photons are indistinguishable, the function  $\psi$  in (3.3) is permutation-invariant w.r.t.  $\tau_1, \dots, \tau_\ell$ .

Under the single-photon state  $|1_\xi\rangle$ , the field operator  $b(t)$ , which is a quantum stochastic process, has zero mean, and whose covariance function is

$$R(t, r) \triangleq \langle 1_\xi | \check{b}(t) \check{b}^\dagger(r) | 1_\xi \rangle = \delta(t - r) \begin{bmatrix} 1 & 0 \\ 0 & 0 \end{bmatrix} + \begin{bmatrix} \xi(r)^* \xi(t) & 0 \\ 0 & \xi(r) \xi(t)^* \end{bmatrix}, \quad t, r \geq t_0.$$

By (2.15), the gauge process is  $\Lambda(t) = \int_{t_0}^t n(r) dr$ , where  $n(t) \triangleq b^*(t)b(t)$  is the number operator for the field. In the case of the single-photon state  $|1_\xi\rangle$  defined in (3.1), the intensity is the mean  $\bar{n}(t) \triangleq \langle 1_\xi | n(t) | 1_\xi \rangle = |\xi(t)|^2$ . Clearly,  $\int_{t_0}^{\infty} \bar{n}(t) dt = 1$ , i.e., there is one photon in the field.

Next, we look at three commonly used single-photon states. Firstly, when  $\xi(t)$  is an exponentially decaying pulse shape

$$\xi(t) = \begin{cases} \sqrt{\beta} e^{-(\frac{\beta}{2} - i\omega_0)t}, & t \geq 0, \\ 0, & t < 0, \end{cases} \quad (3.4)$$

the state  $|1_\xi\rangle$  can describe a single photon emitted from an optical cavity with resonant frequency  $\omega_o$  and damping rate  $\beta$  or a two-level atom with atomic transition frequency  $\omega_o$  and decay rate  $\beta$  [45, 46]. The frequency counterpart of (3.4) is

$$\xi[i\omega] = \sqrt{\frac{\beta}{2\pi}} \frac{1}{\frac{\beta}{2} + i(\omega - \omega_o)}.$$

Secondly, if  $\xi(t)$  is a rising exponential pulse shape

$$\xi(t) = \begin{cases} \sqrt{\beta} e^{(\frac{\beta}{2} + i\omega_o)t}, & t \leq 0, \\ 0, & t > 0, \end{cases} \quad (3.5)$$

in the frequency representation it is

$$\xi[i\omega] = \sqrt{\frac{\beta}{2\pi}} \frac{1}{\frac{\beta}{2} - i(\omega - \omega_o)}. \quad (3.6)$$

where  $\omega_o$  is the carrier frequency of the light field, then on resonance the single-photon state  $|1_\xi\rangle$  is able to fully excite a two-level system if  $\beta = \kappa$ , where  $\kappa$  is the decay rate as introduced in Example 2.2, see, e.g., [20–22, 47]. The single photon with pulse shape (3.4) or (3.5) has Lorentzian lineshape function with the full width at half maximum (FWHM)  $\beta$  [46, 48], which in the *frequency domain* satisfies

$$|\xi[i\omega]|^2 = \frac{1}{2\pi} \frac{\beta}{(\omega - \omega_o)^2 + \left(\frac{\beta}{2}\right)^2},$$

which is [40, (3.28)] with  $F = 1$  (the single-photon case).

Finally, the Gaussian pulse shape can be given by

$$\xi(t) = \left(\frac{\Omega^2}{2\pi}\right)^{\frac{1}{4}} \exp\left(-\frac{\Omega^2}{4}(t - \tau)^2\right), \quad (3.7)$$

where  $\tau$  is the photon peak arrival time. Applying Fourier transform to  $\xi(t)$  in (3.7) we get

$$|\xi[i\omega]|^2 = \frac{1}{\sqrt{2\pi}} \frac{1}{(\Omega/2)} \exp\left(-\frac{\omega^2}{2(\Omega/2)^2}\right).$$

Hence,  $\Omega$  is the frequency bandwidth of the single-photon wavepacket. Actually,

$$\begin{aligned} \xi[i\omega] &= \frac{1}{\left(\frac{\pi}{2}\Omega^2\right)^{1/4}} \exp\left(\omega(i\tau - \frac{\omega}{\Omega^2})\right) \\ &= \frac{1}{\left(\frac{\pi}{2}\Omega^2\right)^{1/4}} \exp\left(-\left(\frac{\omega - i\pi\Omega/2}{\Omega}\right)^2 - \left(\frac{\tau\Omega}{2}\right)^2\right). \end{aligned}$$

Let  $\tau = 0$  and  $\Omega = \sqrt{2}R$ . Then (3.8) becomes

$$\xi[i\omega] = \frac{1}{\pi^{1/4}\sqrt{R}} \exp\left(-\frac{(\omega/R)^2}{2}\right). \quad (3.8)$$

Similarly, (3.7) becomes

$$\xi(t) = \frac{\sqrt{R}}{\pi^{1/4}} \exp\left(-\frac{(Rt)^2}{2}\right). \quad (3.9)$$

(3.8)-(3.9) are the form of the wavefunction of a vacuum state [29, Chapter 4]. In particular, if  $R \neq 1$ , (3.8)-(3.9) are in the form of the wavefunction of a squeezed vacuum state [49, Eqs. (5.3)-(5.4)]. This is not surprising because vacuum states and squeezed vacuum states are coherent states which have Gaussian wave-packets.

In contrast to the full excitation of a two-level atom by a single photon of rising exponential pulse shape (3.5), the maximal excitation probability of a two-level atom by a single photon of Gaussian pulse shape (3.7) is around 0.8 which is achieved at  $\Omega = 1.46\kappa$ , see, e.g., [20–22, 26, 47].

For a mathematical theory of how to generate a single-photon of a prescribed temporal pulse, interested readers may refer to [50]. For physical generation of a single photon of rising exponential pulse shape, interested readers may refer to [14, 44].

**Remark 3.2.** It should be noted that a continuous-mode single-photon state  $|1_\xi\rangle$  discussed above is different from a continuous-mode single-photon *coherent* state  $|\alpha_\xi\rangle$  which can be defined as

$$|\alpha_\xi\rangle \triangleq \exp(\alpha\mathbf{B}^*(\xi) - \alpha^*\mathbf{B}(\xi))|0\rangle, \quad (3.10)$$

where  $\alpha = e^{i\theta} \in \mathbb{C}$ . For  $|\alpha_\xi\rangle$ , although the mean photon number is

$$\langle\alpha_\xi|\mathbf{B}^*(\xi)\mathbf{B}(\xi)|\alpha_\xi\rangle = |\alpha|^2 = 1,$$

which is the same as the single-photon state  $|1_\xi\rangle$ , the mean amplitude is  $\langle\alpha_\xi|\mathbf{B}(\xi)|\alpha_\xi\rangle = \alpha$ . In contrast, the mean amplitude of the single-photon state  $|1_\xi\rangle$  is  $\langle 1_\xi|\mathbf{B}(\xi)|1_\xi\rangle = 0$ . More discussions can be found in [51, Section 2.1], [35, Section 7.1.1]. Finally, continuum coherent states are defined in [40, (3.1) and (3.6)] and [21, (24)], which in our notation are of the form

$$|\{\alpha[i\omega]\}\rangle = \exp\left(\int_{-\infty}^{\infty} d\omega (\alpha[i\omega]b[i\omega]^\dagger - \alpha[i\omega]^*b[i\omega])\right)|0\rangle. \quad (3.11)$$

Clearly, if  $\alpha[i\omega] = \alpha\xi[i\omega]$ , (3.11) becomes (3.10). A time-domain discussion can be found in [47].

If an electromagnetic field is confined for example in a cavity, it will have discrete modes instead of a continuum of modes. Next, we introduce *single-mode* coherent states. If a laser is incident on the cavity, the cavity can be in a coherent state. Moreover, in quantum optics, laser is often assumed to produce a single-mode coherent signal. The reason is simple, if the pulse

$\xi[i\omega] \equiv \gamma\delta[\omega_o]$  in (3.10), where  $\gamma \in \mathbb{R}$  and  $\omega_o$  is the central frequency, then we have a *single-mode* coherent state

$$|\beta\rangle = \exp(\beta b^*[i\omega_o] - \beta^* b[i\omega_o]) |0\rangle, \quad (3.12)$$

where  $\beta = \alpha\gamma \in \mathbb{C}$ . The single-mode coherent state  $|\beta\rangle$  can be rewritten as

$$|\beta\rangle = e^{-\frac{1}{2}|\beta|^2} \sum_{n=0}^{\infty} \frac{\beta^n}{\sqrt{n!}} |n\rangle. \quad (3.13)$$

Clearly, the vacuum state  $|0\rangle$  is a coherent state ( $\beta = 0$  in (3.12)). Another type of single-mode coherent states, single-mode squeezed vacuum states, will be introduced in Section 7. Finally, it is worthwhile to point out that there is a slight abuse of notation in (3.12). In this survey, the annihilation operator of a free propagating field is denoted by  $b(t)$ , while that for a cavity is denoted by  $a(t)$ . However, as we want to show that the single-mode coherent state  $|\beta\rangle$  in (3.12) is an ideal approximation of the continuous-mode coherent state  $|\alpha\xi\rangle$  in (3.10), we feel it is good to use  $b(t)$  in both of these two equations.

More discussions on coherent states can be found in [29, Chapter 4].

**Remark 3.3.** The operator  $\mathbf{B}^*(\xi)$  defined via (3.1) is called a discrete photon creation operator in the temporal modes theory of quantum optics; see e.g., [52, (2.14)] and [53, (7)]. Roughly speaking, under the *narrow-band approximation* as described in Remark 2.1, using  $b[i\omega]$  we can define a time-spatial operator, [45, (7.3)],

$$b(x, t) = e^{-i\omega_o(t-x/c)} \frac{1}{\sqrt{2\pi}} \int_{-\infty}^{\infty} d\omega' b[i\omega'] e^{-i\omega'(t-x/c)},$$

where  $\omega_o$  is the carrier frequency of the free propagating field. Denote

$$\begin{aligned} \mathcal{E}^+(x, t) &= ib(x, t), \\ \mathcal{E}^-(x, t) &= -ib(x, t)^* = (\mathcal{E}^+(x, t))^*. \end{aligned} \quad (3.14)$$

Then in a simplified form, an electromagnetic field propagating along the positive  $x$  direction can be described as, [54],

$$\mathcal{E}(x, t) = \mathcal{E}^+(x, t) + \mathcal{E}^-(x, t) = i(b(x, t) - b(x, t)^*).$$

Let  $\{\xi_j\}$  be an orthonormal basis of the space of the square-integrable pulse shapes  $\xi$ . An example of  $\{\xi_j[i\omega]\}$  is the set of wighted Hermite polynomials [55, Chapter 8]. Define

$$\mathbf{B}_j \triangleq \mathbf{B}(\xi_j) = \int_{-\infty}^{\infty} dt b(t) \xi_j^*(t) = \int_{-\infty}^{\infty} d\omega b[i\omega] \xi_j^*[i\omega].$$

Clearly,  $\mathbf{B}_j^* |0\rangle$  generates a photon of pulse shape  $\xi_j$ . Moreover, as  $\{\xi_j\}$  is an orthonormal basis, we have

$$\sum_j \xi_j[i\omega] \mathbf{B}_j = \int_{-\infty}^{\infty} d\omega' b[i\omega'] \sum_j \xi_j[i\omega] \xi_j^*[i\omega'] \int_{-\infty}^{\infty} d\omega b[i\omega] \delta(\omega - \omega') = b[i\omega]. \quad (3.15)$$

Define a time-spatial function  $\nu_j(x, t)$  which is associated with  $\xi_j$  by

$$\nu_j(x, t) \triangleq ie^{-i\omega_0(t-x/c)} \frac{1}{\sqrt{2\pi}} \int_{-\infty}^{\infty} d\omega' \xi_j[i\omega'] e^{-i\omega'(t-x/c)}. \quad (3.16)$$

By (3.15)-(3.16), the positive-frequency part  $\mathcal{E}^+(x, t)$  of an electromagnetic field defined in (3.14) can be re-written as

$$\mathcal{E}^+(x, t) = \sum_j \nu_j(x, t) \mathbf{B}_j.$$

More discussions can be found in a recent review on temporal modes in quantum optics [53].

### 3.1 Discrete measurement of a continuous-mode single-photon state

In this subsection, we present a procedure of digitizing a continuous-mode single-photon state  $|1_\xi\rangle$  as is proposed in [44].

Assume that the time interval  $(-\infty, \infty)$  is partitioned into time bins of equal length  $\Delta t$  and let  $t_j = j\Delta t$  for  $j = 0, \pm 1, \dots$ . When  $\Delta t$  is sufficiently small, the value of  $\xi(t)$  in the time bin  $[j\Delta t, (j+1)\Delta t)$  is well approximated by  $\xi_{t_j}$ . Then a continuous-mode single-photon state  $|1_\xi\rangle$  can be approximately written as

$$|1_\xi\rangle = \int_{-\infty}^{\infty} \xi^*(t) b^*(t) dt |0\rangle = \sum_j \xi^*(t_j) \frac{1}{\Delta t} \int_{t_j}^{t_{j+1}} b^*(t) dt |0\rangle. \quad (3.17)$$

Denote

$$|1_j\rangle = c_j^* |0\rangle \equiv \frac{1}{\Delta t} \int_{t_j}^{t_{j+1}} b^*(t) dt |0\rangle. \quad (3.18)$$

Notice that

$$[c_j, c_k^*] = \frac{\delta_{jk}}{\Delta t}. \quad (3.19)$$

**Remark 3.4.** According to (3.19),  $[c_j, c_j^*]$  becomes a Dirac delta function  $\delta(t_j)$  in the limit  $\Delta t \rightarrow 0$ . This justifies the coefficient  $\frac{1}{\Delta t}$  in the definition of  $c_j^*$  in (3.18).

By means of (3.18), the approximated single-photon state in (3.17) can be re-written as

$$|1_\xi\rangle = \sum_j \xi^*(t_j) |1_j\rangle.$$

The corresponding density matrix is

$$\rho = |1_\xi\rangle \langle 1_\xi| = \sum_{mn} \rho_{mn} |1_m\rangle \langle 1_n|, \quad (3.20)$$

where  $\rho_{mn} = \xi^*(t_m)\xi(t_n)$ . Define a quadrature  $X_j$  for the  $j$ th time bin to be

$$X_j \triangleq \frac{c_j e^{-i\theta_j} + c_j^* e^{i\theta_j}}{\sqrt{2}} \quad (3.21)$$

where

$$\theta_j = \omega_d \cdot t_j + \theta_0$$

with  $\omega_d$  being the frequency detuning between the central frequency of the signal (the single-photon state  $|1_\xi\rangle$ ) and that of the local oscillator for homodyne measurement, and  $\theta_0$  being the local oscillator's relative phase at  $t = 0$ . As  $X_j = X_j^*$ ,  $X_j$  is an observable which can be measured in principle. Moreover, it can be shown that

$$[X_j, X_k] = -\frac{i\delta_{jk}}{\Delta t} \sin((j-k)\omega_d\Delta t) = 0, \quad j \neq k.$$

The time series  $\{X_j\}$  can be measured in experiments.

**Remark 3.5.** Notice that the quadrature  $X_j$  defined in (3.21) can be re-written as

$$X_j = \frac{c_j + c_j^*}{\sqrt{2}} \cos \theta_j + \frac{c_j - c_j^*}{i\sqrt{2}} \sin \theta_j \equiv Q_j \cos \theta_j + P_j \sin \theta_j,$$

where the quadratures  $Q_j = \frac{c_j + c_j^*}{\sqrt{2}}$  and  $P_j = \frac{c_j - c_j^*}{i\sqrt{2}}$  satisfy

$$[Q_j, P_j] = \frac{i}{\Delta t}.$$

It can be calculated that

$$X_k |1_m\rangle = \frac{e^{-i\theta_k}}{\sqrt{2}} \delta_{km} |0\rangle + \frac{1}{\Delta t} \frac{e^{i\theta_k}}{\sqrt{2}} \int_{t_j}^{t_{j+1}} dt \int_{t_m}^{t_{m+1}} dr b^*(t) b^*(r) |0\rangle. \quad (3.22)$$

Therefore, we have

$$\langle 1_n | X_j X_k | 1_m \rangle = \frac{1}{2} (e^{-i(\theta_k - \theta_j)} \delta_{km} \delta_{jn} + \delta_{jk} \delta_{mn} + e^{-i(\theta_j - \theta_k)} \delta_{jm} \delta_{kn}). \quad (3.23)$$

Let  $I(t_j)$  be the homodyne current for the  $j$ th time bin, which is proportional to  $X_j$ . By (3.20) and (3.23), we have

$$\begin{aligned} \langle I(t_j) I(t_k) \rangle &\propto \langle X_j X_k \rangle \\ &= \text{Tr}[\rho X_j X_k] = \sum_{mn} \rho_{mn} \langle 1_n | X_j X_k | 1_m \rangle \\ &= \frac{1}{2} (e^{-i(\theta_k - \theta_j)} \rho_{kj} + \delta_{jk} + e^{-i(\theta_j - \theta_k)} \rho_{jk}) \\ &= \frac{1}{2} \delta_{jk} + \text{Re}[\rho_{jk}] \cos(\theta_j - \theta_k) + \text{Im}[\rho_{jk}] \sin(\theta_j - \theta_k) \\ &= \frac{1}{2} \delta_{jk} + \text{Re}[\rho_{jk}] \cos(\omega_d(t_j - t_k)) + \text{Im}[\rho_{jk}] \sin(\omega_d(t_j - t_k)), \end{aligned}$$

which is [44, (5)].

**Remark 3.6.** In an experiment, it is the homodyne photocurrent  $I(t)$  that is recorded, from which  $\langle X_j X_k \rangle$  is obtained by averaging over many trajectories. After getting  $\langle X_j X_k \rangle$ ,  $\text{Re}[\rho_{jk}]$  and  $\text{Im}[\rho_{jk}]$  can be retrieved, from which we can get a discrete approximation of  $\xi(t)$ .

## 4 Linear systems' response to single-photon states

Let the system  $G$  in Fig. 1 be linear and driven by  $m$  photons, one in each input field. Also, assume that  $G$  is initialized in a coherent state. Single-mode coherent states are defined in (3.13), its multi-mode counterpart can be found in [56, Section II-E]. In this section, we present the state of the output fields.

Given two constant matrices  $U, V \in \mathbb{C}^{r \times k}$ , a doubled-up matrix  $\Delta(U, V)$  is defined as

$$\Delta(U, V) \triangleq \begin{bmatrix} U & V \\ V^\# & U^\# \end{bmatrix}.$$

Let  $I_k$  be an identity matrix and  $0_k$  a zero square matrix, both of dimension  $k$ . Define  $J_k = \text{diag}(I_k, -I_k)$ . Then for a matrix  $X \in \mathbb{C}^{2j \times 2k}$ , define  $X^\flat = J_k X^\dagger J_j$ . In the linear case, the system  $G$  can be used to model a collection of  $n$  quantum harmonic oscillators that are driven by  $m$  input fields. Denote  $a(t) = [a_1(t) \ \cdots \ a_n(t)]^\top$ , where  $a_j(t)$  is the annihilation operator for the  $j$ th harmonic oscillator,  $j = 1, \dots, n$ . In the  $(S, L, H)$  formalism, the inherent system Hamiltonian is given by  $H = (1/2)\check{a}^\dagger \Omega \check{a}$ , where  $a = [a^\top \ (a^\#)^\top]^\top$ , and  $\Omega = \Delta(\Omega_-, \Omega_+) \in \mathbb{C}^{2n \times 2n}$  is a Hermitian matrix with  $\Omega_-, \Omega_+ \in \mathbb{C}^{n \times n}$ . The coupling between the system and the fields is described by the operator  $L = [C_- \ C_+] \check{a}$ , with  $C_-, C_+ \in \mathbb{C}^{m \times n}$ . Finally, the scattering operator  $S$  is an  $m \times m$  constant matrix such that  $S^\dagger S = S S^\dagger = I_m$ . The dynamics of the open quantum linear system in Fig. 1 are described by the following linear Itô QSDEs ([57, (26)], [56, (14)-(15)], [38, (5)-(6)], [58, 59], [37, Chapter 2]),

$$\begin{aligned} d\check{a}(t) &= Aa(t)dt + Bd\check{B}(t), \\ d\check{B}_{\text{out}}(t) &= Ca(t)dt + Dd\check{B}(t), \quad t \geq t_0, \end{aligned} \tag{4.1}$$

where

$$D = \Delta(S, 0), C = \Delta(C_-, C_+), B = -C^\flat \Delta(S, 0), A = -\frac{1}{2}C^\flat C - iJ_n \Delta(\Omega_-, \Omega_+).$$

These constant system matrices are parametrized by the physical parameters  $\Omega_-, \Omega_+, C_-, C_+$  and satisfy

$$A + A^\flat + BB^\flat = 0, \tag{4.2a}$$

$$B = -C^\flat \Delta(S, 0). \tag{4.2b}$$

(4.2a) is equivalent to

$$[\check{a}(t), \check{a}^\dagger(t)] \equiv [\check{a}(t_0), \check{a}^\dagger(t_0)] = J_n, \quad \forall t \geq t_0.$$

That is, the system variables preserve canonical commutation relations. On the other hand, (4.2b) is equivalent to

$$[\check{a}(t), \check{b}_{\text{out}}^\dagger(r)] = 0, \quad t \geq r \geq t_0.$$



That is, the system variables and the output satisfy the non-demolition condition. In the quantum control literature, equations (4.2a)-(4.2b) are called *physical realization* conditions. Roughly speaking, if these conditions are met, the mathematical model (4.1) could in principle be physically realized ([60], [61]).

Let  $X$  be an operator on the joint system-field space. Denote by  $\langle X(t) \rangle$  the expected value of  $X(t)$  with respect to the initial joint system-field state. Then (4.1) has a corresponding *classical* linear system of the form

$$\begin{aligned} d\langle \check{a}(t) \rangle &= A\langle a(t) \rangle dt + Bd\langle \check{B}(t) \rangle, \\ d\langle \check{B}_{\text{out}}(t) \rangle &= C\langle a(t) \rangle dt + Dd\langle \check{B}(t) \rangle, \quad t \geq t_0, \end{aligned} \quad (4.3)$$

By means of the classical linear systems theory, we can define Hurwitz stability, controllability and observability of a linear quantum system.

**Definition 4.1.** [34, Definition 1] *The quantum linear system (4.1) is said to be Hurwitz stable (resp. controllable, observable) if the corresponding classical linear system (4.3) is Hurwitz stable (resp. controllable, observable).*

Moreover, as in classical linear systems theory, the *impulse response function* for the system  $G$  is defined as

$$g_G(t) \triangleq \begin{cases} \delta(t)D - Ce^{At}C^\dagger D, & t \geq 0, \\ 0, & t < 0. \end{cases} \quad (4.4)$$

It is easy to show that  $g_G(t)$  defined in (4.4) has the following nice structure

$$g_G(t) = \Delta(g_{G^-}(t), g_{G^+}(t)),$$

where

$$\begin{aligned} g_{G^-}(t) &\triangleq \begin{cases} \delta(t)S - [C_- \ C_+]e^{At} \begin{bmatrix} C_-^\dagger \\ -C_+^\dagger \end{bmatrix} S, & t \geq 0 \\ 0, & t < 0 \end{cases}, \\ g_{G^+}(t) &\triangleq \begin{cases} -[C_- \ C_+]e^{At} \begin{bmatrix} -C_+^T \\ C_-^T \end{bmatrix}, & t \geq 0 \\ 0, & t < 0 \end{cases}. \end{aligned}$$

Given a function  $f(t)$  in the time domain, its two-sided Laplace transform [62, Chapter 10] is defined as

$$F[s] \equiv \mathcal{L}_b\{f(t)\}(s) \triangleq \int_{-\infty}^{\infty} e^{-st} f(t) dt.$$

Applying the two-sided Laplace transform to the impulse response function (4.4) yields the transfer function

$$\Xi_G[s] = \Delta(\Xi_{G^-}[s], \Xi_{G^+}[s]),$$

where  $\Xi_{G^-}[s] = \mathcal{L}_b\{g_{G^-}(t)\}(s)$  and  $\Xi_{G^+}[s] = \mathcal{L}_b\{g_{G^+}(t)\}(s)$ .

If  $C^+ = 0$  and  $\Omega^+ = 0$ , the resulting quantum linear system is said to be *passive* [34, 38, 58]. Specifically, the Itô QSDEs for a passive linear quantum system are (e.g., see [34, Sec. 3.1]),

$$\begin{aligned} da(t) &= \mathcal{A}a(t)dt + \mathcal{B}dB(t), \\ dB_{\text{out}}(t) &= \mathcal{C}a(t)dt + \mathcal{D}dB(t), \quad t \geq t_0, \end{aligned} \tag{4.5}$$

where

$$\mathcal{A} = -i\Omega_- - \frac{1}{2}C_-^\dagger C_-, \quad \mathcal{B} = -C_-^\dagger S, \quad \mathcal{C} = C_-, \quad \mathcal{D} = S.$$

An equivalent way to characterize the structure of the passive linear quantum system (4.5) is by the physical realizability conditions

$$\mathcal{A} + \mathcal{A}^\dagger + \mathcal{B}\mathcal{B}^\dagger = 0, \quad \mathcal{B} = -\mathcal{C}^\dagger S.$$

Moreover, in the passive case,  $\Xi_{G^+}[s] \equiv 0$  and

$$\Xi_{G^-}[s] = S - C_-(sI + i\Omega_- + \frac{1}{2}C_-^\dagger C_-)^{-1}C_-^\dagger S.$$

Hence, if a linear system is passive, then its dynamics are completely characterized by its annihilation operators. Moreover, it can be easily verified that

$$\Xi_{G^-}[i\omega]^\dagger \Xi_{G^-}[i\omega] \equiv I_m, \quad \forall \omega \in \mathbb{R}.$$

Hence, an empty cavity does not change the amplitude of the input signal, but modifies its phase.

**Example 4.1** (Re-visit Example 2.1). *For the cavity model in Example 2.1, clearly  $C^+ = 0$ ,  $\Omega^+ = 0$  and  $S = 1$ . In this case  $\Xi_{G^+}[s] \equiv 0$  and*

$$\Xi_{G^-}[s] = \frac{s + i\omega_d - \frac{\kappa}{2}}{s + i\omega_d + \frac{\kappa}{2}}.$$

*As a result, the input-output relation in the frequency domain is*

$$b_{\text{out}}[s] = \frac{s + i\omega_d - \frac{\kappa}{2}}{s + i\omega_d + \frac{\kappa}{2}} b_{\text{in}}[s].$$

Let the linear quantum system  $G$  be initialized in the coherent state  $|\eta\rangle$  and the input field be initialized in the vacuum state  $|0\rangle$ . Then the initial joint system-field state is  $\rho_{0g} \triangleq |\eta\rangle\langle\eta| \otimes |0\rangle\langle 0|$  in the form of a density matrix. Denote

$$\rho_{\infty g} = \lim_{t \rightarrow \infty, t_0 \rightarrow -\infty} U(t, t_0) \rho_{0g} U(t, t_0)^*.$$

Here,  $t_0 \rightarrow -\infty$  indicates that the interaction starts in the remote past and  $t \rightarrow \infty$  means that we are interested in the dynamics in the far future. In other words, we look at the steady-state dynamics. Define

$$\rho_{\text{field,g}} \triangleq \langle \eta | \rho_{\infty g} | \eta \rangle. \quad (4.6)$$

In other words, the system is traced off and we focus on the steady-state state of the output field.

The following result gives the response of a quantum linear system to a single-channel single-photon state.

**Theorem 4.1.** [56, Proposition 2] *Assume there is one input field which is in the single photon state  $|1_\xi\rangle$ . Also, assume that  $G$  is Hurwitz stable and is initialized in a coherent state  $|\eta\rangle$ . Then the steady-state output field state for the linear quantum system  $G$  is*

$$\rho_{\text{out}} = (\mathbf{B}^*(\xi_{\text{out}}^-) - \mathbf{B}(\xi_{\text{out}}^+))\rho_{\text{field,g}}(\mathbf{B}^*(\xi_{\text{out}}^-) - \mathbf{B}(\xi_{\text{out}}^+))^*,$$

where

$$\Delta(\xi_{\text{out}}^-[s], \xi_{\text{out}}^+[s]) = \Xi_G[s]\Delta(\xi[s], 0),$$

and  $\rho_{\text{field,g}}$ , defined in (4.6), is the density operator for the output field with zero mean and covariance function

$$R_{\text{out}}[i\omega] = \Xi_G[i\omega]R_{\text{in}}[i\omega]\Xi_G[i\omega]^\dagger$$

with

$$R_{\text{in}}[i\omega] = \begin{bmatrix} 1 & 0 \\ 0 & 0 \end{bmatrix}.$$

In particular, if the linear system  $G$  is passive and initialized in the vacuum state, then  $\xi_{\text{out}}^+[s] \equiv 0$  and  $R_{\text{out}}[i\omega] \equiv R_{\text{in}}[i\omega]$ . In other words, the steady-state output is a single-photon state  $|1_{\xi_{\text{out}}^-}\rangle$ .

**Example 4.2.** *Let the optical cavity introduced in Example 2.1 be initialized in the vacuum state. Then, by Theorem 4.1, the steady-state output field state is also a single-photon state  $|1_{\xi_{\text{out}}^-}\rangle$  with the pulse shape*

$$\xi_{\text{out}}^-[i\omega] = \frac{i(\omega + \omega_d) - \frac{\kappa}{2}}{i(\omega + \omega_d) + \frac{\kappa}{2}}\xi[i\omega].$$

**Remark 4.1.** It has been shown in [22] that the output field of a two-level atom initialized in the ground state and driven by a single-photon field  $|1_\xi\rangle$  is also a single-photon state  $|1_{\xi_{\text{out}}^-}\rangle$ . Thus, although the dynamics of a two-level atom is bilinear, see Example 2.2, in the single-photon input case it can be fully characterized by a linear systems theory.

If the linear system  $G$  is not passive, or is not initialized in the vacuum state, the steady-state output field state  $\rho_{\text{out}}$  in general is not a single-photon state; as can be seen in Theorem

4.1. This new type of states has been named “photon-Gaussian” states in [56]. Moreover, it has been proved in [56] that the class of “photon-Gaussian” states is invariant under the steady-state action of a linear quantum system. In what follows we present this result.

**Definition 4.2.** [56, Definition 1] A state  $\rho_{\xi,R}$  is said to be a photon-Gaussian state if it belongs to the set

$$\mathcal{F} \triangleq \left\{ \rho_{\xi,R} = \prod_{k=1}^m \sum_{j=1}^m \left( B_j^*(\xi_{jk}^-) - B_j(\xi_{jk}^+) \right) \rho_R \left( \prod_{k=1}^m \sum_{j=1}^m \left( B_j^*(\xi_{jk}^-) - B_j(\xi_{jk}^+) \right) \right)^* \right. \\ \left. : \text{function } \xi = \Delta(\xi^-, \xi^+) \text{ and density matrix } \rho_R \text{ satisfy } \text{Tr}[\rho_{\xi,R}] = 1 \right\}.$$

**Theorem 4.2.** [56, Theorem 5] Let  $\rho_{\xi_{\text{in}}, R_{\text{in}}} \in \mathcal{F}$  be a photon-Gaussian input state. Also, assume that  $G$  is Hurwitz stable and is initialized in a coherent state  $|\eta\rangle$ . Then the linear quantum system  $G$  produces in steady state a photon-Gaussian output state  $\rho_{\xi_{\text{out}}, R_{\text{out}}} \in \mathcal{F}$ , where

$$\begin{aligned} \xi_{\text{out}}[s] &= \Xi_G[s] \xi_{\text{in}}[s], \\ R_{\text{out}}[i\omega] &= \Xi_G[i\omega] R_{\text{in}}[i\omega] \Xi_G[i\omega]^\dagger. \end{aligned}$$

Next, we present a result for the passive case, which is a special case of Theorem 4.2.

Let the  $k$ th input channel be in a single photon state  $|1_{\mu_k}\rangle$ ,  $k = 1, \dots, m$ . Thus, the state of the  $m$ -channel input is given by the tensor product

$$|\Psi_\mu\rangle = |1_{\mu_1}\rangle \otimes \cdots \otimes |1_{\mu_m}\rangle. \quad (4.7)$$

Denote  $\mu = [\mu_1 \ \cdots \ \mu_m]^\top$ .

**Corollary 4.1.** Assume that the passive linear quantum system (4.5) is Hurwitz stable, initialized in the vacuum state and driven by an  $m$ -photon input state  $|\Psi_\mu\rangle$ . The the steady-state output state is another  $m$ -photon  $|\Psi_\nu\rangle$  whose pulse  $\nu = [\nu_1 \ \cdots \ \nu_m]^\top$  is given by

$$\nu[i\omega] = \Xi_{G^-}[i\omega] \mu[i\omega].$$

Response of quantum linear systems to multi-photon states has been studied in [63, 64]. In particular, the multi-photon versions of Corollary 4.1 can be found in [63, Corollary 11] and [64, Theorems 2-7]. Response of quantum nonlinear systems to multi-photon states has been studied in [22, 28, 54].

We end this section with a final remark.

**Remark 4.2.** To derive the output pulse shapes of a quantum linear system  $G$  driven by continuous-mode single- or multiple-photon states, it is assumed in [56, 63, 64] that the system  $G$  is Hurwitz stable. Actually, if the system  $G$  is passive, the results also hold even if  $G$  is marginally

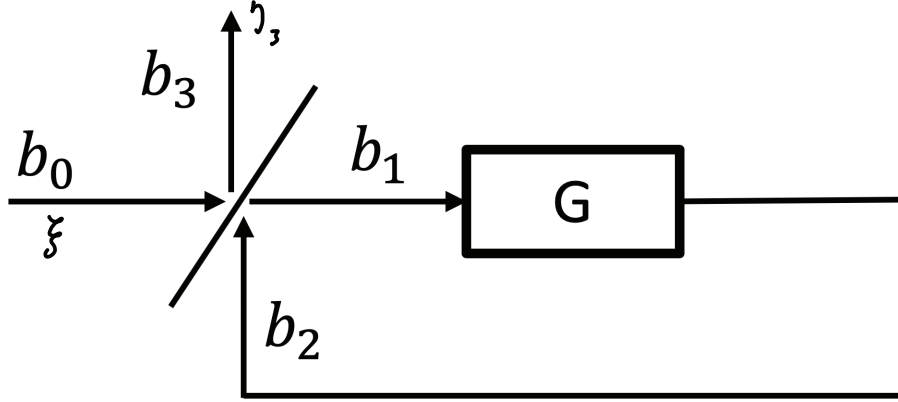


Figure 2: Linear quantum coherent feedback network composed of an empty cavity and a beam-splitter. The input field  $b_0$  is in the single photon state  $|1_\xi\rangle$  and the output field  $b_3$  is in the single-photon output state  $|1_{\eta_3}\rangle$

stable. The reason is the following. By [38, Corollary 4.1], a passive quantum linear system can only have a  $co$  subsystem which is both controllable and observable, and a  $\bar{c}\bar{o}$  subsystem which is neither controllable nor observable. Actually, the  $\bar{c}\bar{o}$  subsystem is a closed system, and hence the modes related to the  $\bar{c}\bar{o}$  subsystem will not affect system's input-output behavior. As the system is passive, by [38, Corollary 4.1], the  $\bar{c}\bar{o}$  subsystem exactly corresponds to the subsystem whose poles are on the imaginary axis, and all the poles of the  $co$  subsystem lie on the open left half of the complex plane, which means that the  $co$  subsystem is Hurwitz stable, and thus all the results in [56, 63, 64] still hold.

## 5 Single-photon pulse shaping via coherent feedback

In this section, based on the development in Section 4, we demonstrate how a quantum linear coherent feedback network can be constructed to manipulate the temporal pulse shape of a single-photon input state.

If a cavity, as given in Example 2.1, is driven by a single-photon state  $|1_\xi\rangle$ , by Example 4.2 the output pulse shape in the frequency domain is

$$\eta_1[i\omega] = \frac{i(\omega + \omega_d) - \frac{\kappa}{2}}{i(\omega + \omega_d) + \frac{\kappa}{2}} \xi[i\omega]. \quad (5.1)$$

Now we put the cavity into a coherent feedback network closed by a beamsplitter, as shown in Fig. 2. (Here, the word ‘‘coherent’’ indicates that no measurement is involved in the feedback

loop and thus all the signals remain quantum). Let the beamsplitter be

$$S_{\text{BS}} = \begin{bmatrix} \sqrt{\gamma} & \sqrt{1-\gamma} \\ -\sqrt{1-\gamma} & \sqrt{\gamma} \end{bmatrix}, \quad 0 \leq \gamma \leq 1.$$

Clearly, the beamsplitter  $S_{\text{BS}}$  is a special passive linear system (4.5) whose system parameters are

$$\mathcal{A} = \mathcal{B} = \mathcal{C} = 0, \quad \mathcal{D} = S_{\text{BS}}.$$

Thus, the input-output relation for the beamsplitter  $S_{\text{BS}}$  is

$$\begin{bmatrix} b_3 \\ b_1 \end{bmatrix} = S_{\text{BS}} \begin{bmatrix} b_0 \\ b_2 \end{bmatrix}.$$

Clearly, the feedback network from input  $b_0$  to output  $b_3$  in Fig. 2 is still a quantum linear passive system that is driven by the single-photon state  $|1_\xi\rangle$  for the input field  $b_0$ . By the development in Section 4, we can get the pulse shape for the output field  $b_3$ , which is

$$\eta_3[i\omega] = \frac{-\frac{1-\sqrt{\gamma}}{1+\sqrt{\gamma}}(\omega + \omega_d)i + \frac{\kappa}{2}}{\frac{1-\sqrt{\gamma}}{1+\sqrt{\gamma}}(\omega + \omega_d)i + \frac{\kappa}{2}} \xi[i\omega].$$

Fix  $\beta = 2$  for the exponentially decaying single-photon state in (3.4), and  $\omega_d = 0$  and  $\kappa = 2$  for the optical cavity in Example 2.1. The *temporal* pulse shapes  $\xi(t)$ ,  $\eta_1(t)$  and  $\eta_3(t)$  are plotted in Fig. 3.

Fix  $\tau = 0$  and  $\Omega = 1.46$  for a Gaussian single-photon state in (3.7), and  $\omega_d = 0$  and  $\kappa = 1$  for the optical cavity. When  $\xi(t)$  is of a Gaussian pulse shape (3.7) for the optical cavity in Example 2.1. The *temporal* pulse shapes  $\xi(t)$ ,  $\eta_1(t)$  and  $\eta_3(t)$  are plotted in Fig. 4.

## 6 Single-photon filter and master equation

As discussed in Section 3, a single-photon light field has statistical properties. Therefore, it is natural to study the filtering problem of a quantum system driven by a single-photon field state. Single-photon filters were first derived in [24, 65], and their multi-photon version was developed in [26, 27, 66]. In this section, we focus on the single-photon case. The basic setup is given in Fig. 5.

The output field of an open quantum system can be continuously measured, see for example Subsection 3.1; based on the measurement data a quantum filter can be built to estimate some quantity of the system. For example, we desire to know which state a two-level atom is in, the ground state  $|g\rangle$  or the excited state  $|e\rangle$ . Unfortunately, it is not realistic to measure the state of the atom directly. Instead, a light field may be impinged on the atom and from the scattered

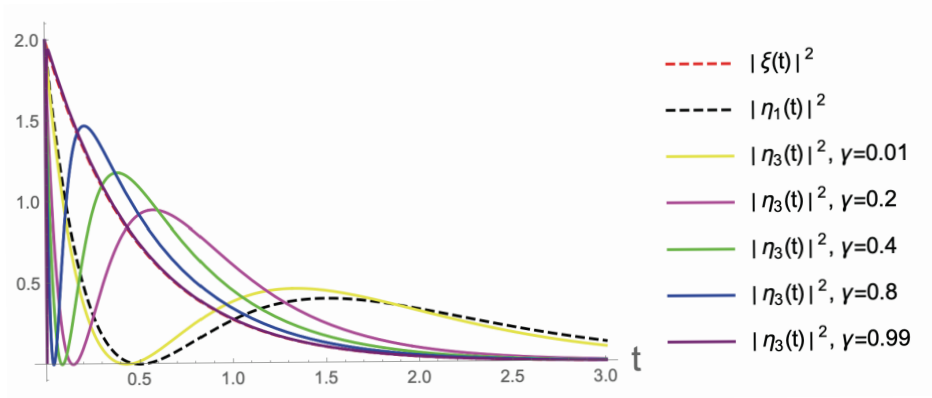


Figure 3:  $|\xi(t)|^2$  is the detection probability of the input single photon,  $|\eta_1(t)|^2$  is the detection probability of the output photon in the case of the cavity,  $|\eta_3(t)|^2$  are the detection probabilities of the output photon in the linear coherent feedback network (Fig. 2) with various beamsplitter parameter  $\gamma$ .

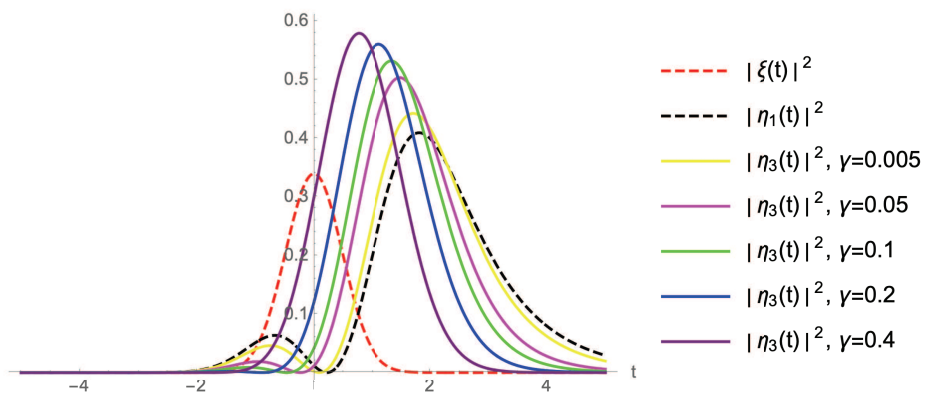


Figure 4: The same as those in Fig. 3.

light we estimate the state of the atom. Homodyne detection and photon-counting measurements are the two most commonly used measurement methods in quantum optical experiments. In this survey, we focus on Homodyne detection as discussed in Subsection 3.1. In Fig. 5,  $G$  is a quantum system which is driven a single photon of pulse shape  $\xi$ . After interaction, the output field, represented by its integrated annihilation operator  $B_{\text{out}}$  and creation operator  $B_{\text{out}}^*$ , is also in a single-photon state with pules shape  $\eta$ . Due to measurement imperfection (measurement inefficiency), the output field  $|1_\eta\rangle$  may be contaminated [12,67]. This is usually mathematically modeled by mixing  $|1_\eta\rangle$  with an additional quantum vacuum through a beam splitter, as shown in Fig. 5. The beam splitter in Fig. 5 is of a general form

$$S_{\text{BS}} = \begin{bmatrix} s_{11} & s_{12} \\ s_{21} & s_{22} \end{bmatrix} \quad (6.1)$$

where  $s_{ij} \in \mathbb{C}$ . As a result, there are two final output fields, which are

$$\begin{bmatrix} B_{1,\text{out}} \\ B_{2,\text{out}} \end{bmatrix} = S_{\text{BS}} \begin{bmatrix} B_{\text{out}} \\ B_v \end{bmatrix},$$

where  $B_v$  is the integrated annihilation operator for the additional quantum noise channel. The quadratures of the outputs are continuously measured by homodyne detectors, which are given by

$$Y_1(t) = B_{1,\text{out}}(t) + B_{1,\text{out}}^*(t), \quad Y_2(t) = -i(B_{2,\text{out}}(t) - B_{2,\text{out}}^*(t)). \quad (6.2)$$

In other words, the amplitude quadrature of the first output field is measured, while for the second output field the phase quadrature is monitored.  $Y_i(t)$  ( $i = 1, 2$ ) enjoy the self-non-demolition property

$$[Y_i(t), Y_j(r)] = 0, \quad t_0 \leq r \leq t, \quad i, j = 1, 2,$$

and the non-demolition property

$$[X(t), Y_i(r)] = 0, \quad t_0 \leq r \leq t, \quad i = 1, 2,$$

where  $t_0$  is the time when the system and field start interaction. The quantum conditional expectation is defined as

$$\pi_t(X) \triangleq \mathbb{E}[j_t(X)|\mathcal{Y}_t],$$

where  $\mathbb{E}$  denotes the expectation with respect to the initial joint system-field state,  $j_t(X)$  is given in (2.17), and the commutative von Neumann algebra  $\mathcal{Y}_t$  is generated by the past measurement observations  $\{Y_1(s), Y_2(s) : t_0 \leq s \leq t\}$ . The *conditioned* system density operator  $\rho(t)$  can be obtained by means of  $\pi_t(X) = \text{Tr}[\rho(t)^\dagger X]$ . It turns out that  $\rho(t)$  is a solution to a system of stochastic differential equations, which is called the *quantum filter* in the quantum control community or *quantum trajectories* in the quantum optics community. quantum filtering theory



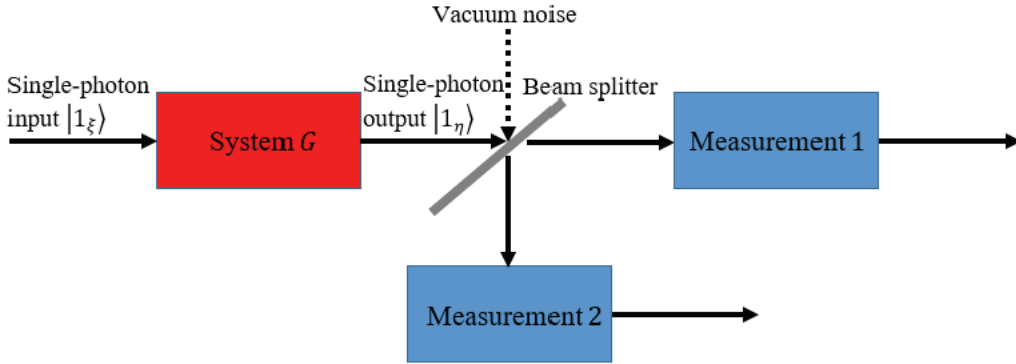


Figure 5: Single-photon filtering. The system of interest  $G$  is driven by a single-photon field state  $|1_\xi\rangle$ . The output single-photon state is denoted by  $|1_\eta\rangle$ . To account for the imperfectness of experiment [67], a beamsplitter is added which mixes  $|1_\eta\rangle$  with a vacuum noise. Both of the signals in the output ports of the beamsplitter are measured to improving the filtering effect.

was pioneered by Belavkin in the early 1980s [68]. More developments can be found in [26, 27, 31, 35, 65, 66, 69–79] and references therein.

In the extreme case that  $S_{\text{BS}}$  is a 2-by-2 identity matrix, the single-photon state  $|1_\eta\rangle$  and the vacuum noise are not mixed and  $|1_\eta\rangle$  is directly measured by “Measurement 1”. This is the case that the output of the two-level system  $G$  is perfectly measured. In this scenario, a quantum filter constructed based on “Measurement 1” is sufficient for the estimation of conditioned system dynamics, as constructed in [24, 65]. However, for a general beam splitter of the form (6.1), the output of the two-level system  $G$  is contaminated by vacuum noise, using two measurements may improve estimation efficiency, as investigated in [80].

The single-photon filter for the set-up in Fig. 5 is given by the following result.

**Theorem 6.1.** [80, Corollary 6.1] *Let the quantum system  $G = (S, L, H)$  in Fig. 5 be initialized in the state  $|\eta\rangle$  and driven by a single-photon input field  $|1_\xi\rangle$ . Assume the output fields are under two homodyne detection measurements (6.2). Then the quantum filter in the Schrödinger picture*

is given by

$$\begin{aligned}
& d\rho^{11}(t) \\
&= \{ \mathcal{L}_G^* \rho^{11}(t) + [S\rho^{01}(t), L^\dagger] \xi(t) + [L, \rho^{10}(t)S^\dagger] \xi^*(t) + (S\rho^{00}(t)S^\dagger - \rho^{00}(t)) |\xi(t)|^2 \} dt \\
&\quad + [s_{11}^* \rho^{11}(t)L^\dagger + s_{11}L\rho^{11}(t) + s_{11}^* \rho^{10}(t)S^\dagger \xi^*(t) + s_{11}S\rho^{01}(t)\xi(t) - \rho^{11}(t)k_1(t)] dW_1(t) \\
&\quad + [is_{21}^* \rho^{11}(t)L^\dagger - is_{21}L\rho^{11}(t) + is_{21}^* \rho^{10}(t)S^\dagger \xi^*(t) - is_{21}S\rho^{01}(t)\xi(t) - \rho^{11}(t)k_2(t)] dW_2(t), \\
& d\rho^{10}(t) \\
&= \{ \mathcal{L}_G^* \rho^{10}(t) + [S\rho^{00}(t), L^\dagger] \xi(t) \} dt \\
&\quad + [s_{11}^* \rho^{10}(t)L^\dagger + s_{11}L\rho^{10}(t) + s_{11}S\rho^{00}(t)\xi(t) - \rho^{10}(t)k_1(t)] dW_1(t) \\
&\quad + [is_{21}^* \rho^{10}(t)L^\dagger - is_{21}L\rho^{10}(t) - is_{21}S\rho^{00}(t)\xi(t) - \rho^{10}(t)k_2(t)] dW_2(t), \\
& d\rho^{00}(t) \\
&= \mathcal{L}_G^* \rho^{00}(t) dt + [s_{11}^* \rho^{00}(t)L^\dagger + s_{11}L\rho^{00}(t) - \rho^{00}(t)k_1(t)] dW_1(t) \\
&\quad + [is_{21}^* \rho^{00}(t)L^\dagger - is_{21}L\rho^{00}(t) - \rho^{00}(t)k_2(t)] dW_2(t), \\
& \rho^{01}(t) = (\rho^{10}(t))^\dagger,
\end{aligned} \tag{6.3}$$

where  $dW_j(t) = dY_j(t) - k_j(t)dt$  with

$$\begin{aligned}
k_1(t) &= s_{11} \text{Tr}[L\rho^{11}(t)] + s_{11}^* \text{Tr}[L^\dagger \rho^{11}(t)] + s_{11} \text{Tr}[S\rho^{01}(t)] \xi(t) \\
&\quad + s_{11}^* \text{Tr}[S^\dagger \rho^{10}(t)] \xi^*(t), \\
k_2(t) &= -is_{21} \text{Tr}[L\rho^{11}(t)] + is_{21}^* \text{Tr}[L^\dagger \rho^{11}(t)] \\
&\quad - is_{21} \text{Tr}[S\rho^{01}(t)] \xi(t) + is_{21}^* \text{Tr}[S^\dagger \rho^{10}(t)] \xi^*(t).
\end{aligned}$$

The initial conditions are  $\rho^{11}(t_0) = \rho^{00}(t_0) = |\eta\rangle\langle\eta|$ ,  $\rho^{10}(t_0) = \rho^{01}(t_0) = 0$ .

**Remark 6.1.** If the beamsplitter  $S_{\text{BS}}$  is a 2-by-2 identity matrix, the single-photon filter (6.3) in Theorem 6.1 reduces to

$$\begin{aligned}
d\rho^{11}(t) &= \left\{ \mathcal{L}_G^* \rho^{11}(t) + [\rho^{01}(t), L^\dagger] \xi(t) + [L, \rho^{10}(t)] \xi^*(t) \right\} dt \\
&\quad + \left[ \rho^{11}(t)L^\dagger + L\rho^{11}(t) + \rho^{10}(t)\xi^*(t) + \rho^{01}(t)\xi(t) - \rho^{11}(t)k_1(t) \right] dW_1(t) \\
d\rho^{10}(t) &= \left\{ \mathcal{L}_G^* \rho^{10}(t) + [\rho^{00}(t), L^\dagger] \xi(t) \right\} dt \\
&\quad + \left[ \rho^{10}(t)L^\dagger + L\rho^{10}(t) + \rho^{00}(t)\xi(t) - \rho^{10}(t)k_1(t) \right] dW_1(t), \\
d\rho^{00}(t) &= \mathcal{L}_G^* \rho^{00}(t) dt + \left[ \rho^{00}(t)L^\dagger + L\rho^{00}(t) - \rho^{00}(t)k_1(t) \right] dW_1(t), \\
\rho^{01}(t) &= (\rho^{10}(t))^\dagger,
\end{aligned} \tag{6.4}$$

where  $dW_1(t)$  and the initial conditions are the same as those in Theorem 6.1, and

$$k_1(t) = \text{Tr}[(L + L^\dagger)\rho^{11}(t)] + \text{Tr}[\rho^{01}(t)]\xi(t) + \text{Tr}[\rho^{10}(t)]\xi^*(t).$$

The filter (6.4) is the quantum single-photon filter first proposed in [24].

Quantum filters describe the joint system-field dynamics conditioned on measurement outputs; On the other hand, if the output field is traced out, we can get the master equation which describes the system dynamics. Master equations are regarded as unconditional system dynamics, see e.g., [24, 31, 73]. Setting  $S = I$  and tracing over the noise terms (represented by  $dW_1(t)$  and  $dW_2(t)$ ) in the quantum filters (6.3) and (6.4), we get the single-photon master equations in the Schrödinger picture

$$\begin{aligned}
\dot{\varrho}^{11}(t) &= \mathcal{L}_G^* \varrho^{11}(t) + [\varrho^{01}(t), L^\dagger] \xi(t) + [L, \varrho^{10}(t)] \xi^*(t), \\
\dot{\varrho}^{10}(t) &= \mathcal{L}_G^* \varrho^{10}(t) + [\varrho^{00}(t), L^\dagger] \xi(t), \\
\dot{\varrho}^{00}(t) &= \mathcal{L}_G^* \varrho^{00}(t), \\
\varrho^{01}(t) &= (\varrho^{10}(t))^\dagger
\end{aligned} \tag{6.5}$$

with initial conditions  $\varrho^{11}(t_0) = \varrho^{00}(t_0) = |\eta\rangle\langle\eta|$ ,  $\varrho^{10}(t_0) = \varrho^{01}(t_0) = 0$ , where

$$\text{Tr}[\varrho^{jk}(t)^\dagger X] = \langle \eta \phi_j | j_t(X) | \eta \phi_k \rangle, \quad j, k = 0, 1$$

with

$$|\phi_j\rangle = \begin{cases} |0\rangle, & j = 0, \\ |1_\xi\rangle, & j = 1. \end{cases}$$

The dynamics of a two-level atom driven by a single photon input field of Gaussian pulse shape has been studied intensively in the literature. In particular, when the photon has a Gaussian pulse shape (3.7) with  $\Omega = 1.46\kappa$ , where  $\kappa$  is the decay rate of the two-level atom; see Example 2.2, it is shown that the maximal excitation probability is around 0.8, see, e.g., [20], [23], [21, Fig. 1], [24, Fig. 8], and [25, Fig. 2]. Recently, the analytical expression of the pulse shape of the output single photon has been derived in [22], which is  $\eta_1$  is (5.1). Assume the Gaussian pulse shape in (3.7) has parameters  $\tau = 3$  and  $\Omega = 1.46\kappa$ . It can be easily verified that  $\int_{-\infty}^4 (|\xi(\tau)|^2 - |\eta_1(\tau)|^2) d\tau = 0.8$ . Interestingly, the excitation probability achieves its maximum 0.8 at time  $t = 4$  (the upper limit of the above integral). Therefore, the filtering result is consistent with that of the input-output response.

## 7 Schrödinger cat states generation

Discussions in the previous sections are for continuous-mode *single-photon* states. In this section, we briefly discuss multi-photon states. In fact, a beamsplitter, which is a very simple linear quantum system but extremely widely used in optics, is able to entangle two input photons (one in each input port) such that two photons can coexist in a single output port. In other words, a 2-photon state is generated. A general theory of multi-photon processing by quantum linear systems has been developed in [63, 64]. In this section, we show how this theory can be applied to generate Schrödinger cat states.

Single-mode coherent states are defined in (3.13). A Schrödinger cat state is a superposition state of two coherent states of opposite phase,  $|\beta\rangle$  and  $|\beta\rangle$ . For example, the odd cat state is

$$\begin{aligned} |\psi\rangle &\triangleq \mathcal{N}_-(|\beta\rangle - |-\beta\rangle) = \mathcal{N}_- e^{-\frac{|\beta|^2}{2}} \sum_{n=0}^{\infty} \frac{2\beta^{2n+1}}{\sqrt{(2n+1)!}} |2n+1\rangle \\ &= \sum_{n=0}^{\infty} \gamma_{\text{cat},n} |2n+1\rangle, \end{aligned}$$

where  $\mathcal{N}_- = \frac{1}{\sqrt{2(1-e^{-2|\beta|^2})}}$  normalizes the odd cat state  $|\psi\rangle$ , and the amplitudes

$$\gamma_{\text{cat},n} \triangleq \mathcal{N}_- e^{-\frac{|\beta|^2}{2}} \frac{2\beta^{2n+1}}{\sqrt{(2n+1)!}}.$$

The bigger  $|\beta|$  is, the larger the cat is. Applications of Schrödinger cat states in quantum teleportation, quantum computation, and quantum metrology can be found in e.g., [81–83]. A scheme for generating Schrödinger cat states is proposed in [67]. In what follows, we use the linear systems theory developed in [56, 63, 64] to derive the main equations in [67].

A single-channel continuous-mode  $\ell$ -photon state  $|\psi_\ell\rangle$  can be defined as

$$|\psi_\ell\rangle \triangleq \frac{1}{\sqrt{N_\ell}} \prod_{k=1}^{\ell} \mathbf{B}^*(\xi_k) |0\rangle,$$

where  $N_\ell$  is the normalization coefficient. If  $\xi_1(t) \equiv \dots \equiv \xi_\ell(t) \equiv \xi(t)$ , then this state is called *continuous-mode* Fock state which has been intensely studied, see e.g., [84, (3)]; [25, (13)]. If we forget the pulse shapes, we can use

$$|n\rangle = \frac{1}{\sqrt{n!}} (\mathbf{B}^*(\xi))^n |0\rangle, \quad \|\xi\|_2 = 1$$

to denote an  $n$ -photon Fock state. In this manner, an  $m$ -channel multi-photon tensor product state is of the form

$$|\Psi\rangle = |n_1\rangle \otimes |n_2\rangle \otimes \dots \otimes |n_m\rangle,$$

where the  $j$ th channel contains  $n_i$  photons.

Consider a beamsplitter of the form

$$S = \begin{bmatrix} T & -R \\ R & T \end{bmatrix}, \quad (R, T \in \mathbb{R}, \quad R^2 + T^2 = 1). \quad (7.1)$$

By [63, Corollary 11 or Example 3], it can be derived that the beamsplitter (7.1) maps a product state  $|n_1\rangle \otimes |n_2\rangle$  to an entangled output state

$$\begin{aligned} &|\Psi_{\text{out}}\rangle \quad (7.2) \\ &= \frac{1}{\sqrt{n_1!n_2!}} \sum_{j=0}^{n_1} \sum_{k=0}^{n_2} \binom{n_1}{j} \binom{n_2}{k} \\ &\quad (-1)^k T^{n_2+j-k} R^{n_1-j+k} \sqrt{(j+k)!(n_1+n_2-j-k)!} |j+k\rangle |n_1+n_2-j-k\rangle. \end{aligned}$$

An ideal single-mode squeezed vacuum state can be expressed as

$$\hat{S}(\eta) |0\rangle = \frac{1}{\sqrt{\cosh \eta}} \sum_{n=0}^{\infty} \alpha_{2n} |2n\rangle, \quad (7.3)$$

where

$$\alpha_{2n} = \frac{\sqrt{(2n)!}}{2^n n!} (-e^{i\phi})^n \tanh^n \eta$$

with  $\eta \in \mathbb{R}$  being the squeezing ratio. In this article, we choose the squeezing angle  $\phi = \pi$  for simplicity. Then  $\alpha_{2n} \in \mathbb{R}$ . More discussions of squeezed states can be found in [46, Chapter 5], [29, Chapter 10], [49], [85], [86], and [87]. According to (7.2), the beamsplitter (7.1) maps  $|\ell\rangle \otimes \hat{S}(\eta) |0\rangle$  to

$$\begin{aligned} |\Psi_{\text{out}}\rangle &= \sum_{n=0}^{\infty} \frac{\alpha_{2n}}{\sqrt{\ell!(2n)!}} \sum_{i=0}^{\ell} \sum_{j=0}^{2n} \binom{\ell}{i} \binom{2n}{2n-j} \\ &\quad \sqrt{(\ell+j-i)!(2n+i-j)!} (-1)^j T^{2n+\ell-i-j} R^{i+j} |\ell+j-i\rangle \otimes |2n+i-j\rangle. \end{aligned} \quad (7.4)$$

Let  $\ell = 0$ , i.e., the first input channel is in the vacuum state. In this case,  $|\Psi_{\text{out}}\rangle$  in (7.4) in a density matrix form is

$$\begin{aligned} \hat{\rho} &= |\Psi_{\text{out}}\rangle \langle \Psi_{\text{out}}| \\ &= \sum_{n,b=0}^{\infty} \alpha_{2n} \alpha_{2b}^* \sum_{j_1=0}^{2n} \sum_{j_2=0}^{2b} \sqrt{\binom{2n}{2n-j_1} \binom{2b}{2b-j_2}} (-1)^{j_1+j_2} T^{2(n+b)-(j_1+j_2)} R^{j_1+j_2} \\ &\quad |j_1\rangle |2n-j_1\rangle \langle 2b-j_2| \langle j_2|. \end{aligned} \quad (7.5)$$

If  $k$  photons are subtracted in the **first** output channel, then by (7.5) the unnormalized conditional state in the second output channel is

$$\begin{aligned} &\text{Tr}_1\{\hat{\rho}\} \\ &= \sum_{k=0}^{\infty} \langle k| \hat{\rho} |k\rangle \\ &= \sum_{n,b=0}^{\infty} \alpha_{2n} \alpha_{2b}^* \sum_{k=0}^{\min\{2n,2b\}} \sqrt{\binom{2n}{2n-k} \binom{2b}{2b-k}} T_1^{2(n+b-k)} R_1^{2k} |2n-k\rangle \langle 2b-k|, \end{aligned}$$

which is  $\hat{\rho}_{t_1}$  in [67, (5)]. Actually,  $\hat{\rho}_{t_1}$  is an *impure* squeezed vacuum state; which accounts for experimental imperfection when an ideal squeezed vacuum state (7.3) is used to generate a Schrödinger cat state; see the red box in [67, Fig. 1]. Next, we derive the output density matrix which is the output of the green box in [67, Fig. 1]. Define

$$\begin{aligned} \rho_{\text{in},2} &= |\ell\rangle \langle \ell| \otimes \hat{\rho}_{t_1} \\ &= \sum_{n,b=0}^{\infty} \alpha_{2n} \alpha_{2b}^* \sum_{k=0}^{\min\{2n,2b\}} \sqrt{\binom{2n}{2n-k} \binom{2b}{2b-k}} T_1^{2(n+b-k)} R_1^{2k} \\ &\quad |\ell\rangle |2n-k\rangle \langle 2b-k| \langle \ell|. \end{aligned}$$

In particular, if  $\ell = 0$ , then  $\rho_{\text{in},2}$  is the input to the beamsplitter in the green box in [67, Fig. 1]. According to (7.2), this beamsplitter maps the pure state  $|\ell\rangle \otimes |2n - k\rangle$  to

$$\begin{aligned} & |\Psi_{2n-k,\ell}\rangle \\ &= \frac{1}{\sqrt{\ell!(2n-k)!}} \sum_{j=0}^{\ell} \sum_{i=0}^{2n-k} \binom{\ell}{j} \binom{2n-k}{i} (-1)^i \\ & R_2^{\ell-j+i} T_2^{2n-k+j-i} \sqrt{(j+i)!(\ell+2n-k-j-i)!} |j+i\rangle |\ell+2n-k-j-i\rangle. \end{aligned}$$

Consequently, the beamsplitter maps the input state  $\rho_{\text{in},2}$  to an output state of the form

$$\begin{aligned} & \rho_{\text{out},2} \\ &= \sum_{n,b=0}^{\infty} \alpha_{2n} \alpha_{2b}^* \sum_{k=0}^{\min\{2n,2b\}} \sqrt{\binom{2n}{2n-k} \binom{2b}{2b-k}} T_1^{2(n+b-k)} R_1^{2k} |\Psi_{2n-k,\ell}\rangle \langle \Psi_{2b-k,\ell}|. \end{aligned}$$

In particular, let  $\ell = 0$ . If we measure the first output channel and detect  $m$  photons, then the unnormalized reduced density matrix is

$$\begin{aligned} & \langle m | \rho_{\text{out},2} | m \rangle \\ &= \sum_{n,b=0}^{\infty} \alpha_{2n} \alpha_{2b}^* \sum_{k=0}^{\min\{2n,2b\}-m} \sqrt{\binom{2n}{2n-k} \binom{2b}{2b-k}} T_1^{2(n+b-k)} R_1^{2k} \\ & \frac{1}{\sqrt{(2n-k)!(2b-k)!}} \binom{2b-k}{m} \binom{2n-k}{m} R_2^{2m} T_2^{2(n+b-k-m)} m! \\ & \sqrt{(2b-k-m)!(2n-k-m)!} |2n-k-m\rangle \langle 2b-k-m| \\ &= \sum_{n,b=0}^{\infty} \alpha_{2n} \alpha_{2b}^* \sum_{k=0}^{\min\{2n,2b\}-m} \sqrt{\binom{2n}{2n-k} \binom{2b}{2b-k}} T_1^{2(n+b-k)} R_1^{2k} \\ & \sqrt{\binom{2b-k}{m} \binom{2n-k}{m}} R_2^{2m} T_2^{2(n+b-k-m)} |2n-k-m\rangle \langle 2b-k-m| \\ &= \sum_{n,b=0}^{\infty} \sum_{k=0}^{\min\{2n,2b\}-m} \frac{\alpha_{2n} \alpha_{2b}^* R_1^{2k} R_2^{2m} (T_1 T_2)^{2(n+b-k)} T_2^{-2m}}{k! m!} \\ & \sqrt{\frac{(2n)!(2b)!}{(2n-k-m)!(2b-k-m)!}} |2n-k-m\rangle \langle 2b-k-m|. \end{aligned} \tag{7.6}$$

**Remark 7.1.** Let  $t_k = T_k^2$  and  $r_k = R_k^2$ ,  $k = 1, 2$ .  $\langle m | \rho_{\text{out},2} | m \rangle$  in (7.6) becomes [67, (11)], whose normalized version is the output density matrix of the green box in [67, Fig. 1]. (The term  $T_2^{-2m}$  is missing in [67, Fig. 1], which is a typo.)

**Remark 7.2.** Many schemes like those proposed in [88–97] that generate Schrödinger cat states can be described uniformly in the mathematical framework similar to that discussed above.

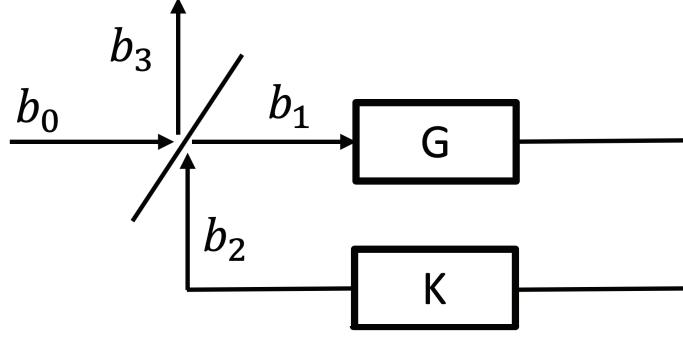


Figure 6: Linear quantum feedback network

## 8 Concluding remarks

In this section, we discuss two possible future research directions.

In [54], Milburn investigated the response of an optical cavity to a continuous-mode single photon, where frequency modulation applied to the cavity is used to engineer the temporal output pulse shape. As frequency modulation involves a time-varying function, the transfer function approach in [56] is not directly applicable. However, it appears that the general procedure outlined in the proof of Proposition 2 and Theorem 5 in [56] can be generalized to the time-varying, yet still linear, case. For example, if the quantum linear passive controller  $K$  in Fig. 6 is allowed to be time-varying, can the output single-photon pulse shape be engineered satisfactorily? This may be a future research direction.

In [98], the authors discussed how to use a single-photon input state to excite one of the two double quantum dot (DQD) qubits which are in a coherent feedback network; see Fig. 1 in [98]. A master equation of the form (6.5) is used to describe the reduced dynamics of the system. By tracing over the cavity and the 2nd DQD qubit, the reduced density operator for the target DQD qubit is given by

$$\rho_{\text{DQD}_1}(t) = \langle g_{20} | \rho^{11}(t) | g_{20} \rangle + \langle g_{21} | \rho^{11}(t) | g_{21} \rangle + \langle e_{20} | \rho^{11}(t) | e_{20} \rangle + \langle e_{21} | \rho^{11}(t) | e_{21} \rangle, \quad (8.1)$$

which is [98, (45)]. Let the initial state of the two DQD qubits be the ground states  $|g_1\rangle$  and  $|g_2\rangle$  and the cavity be initially empty. The purpose of control is to flip the first DQD qubit to its excited state  $|e_1\rangle$  at some time instance  $T$ , by means of designing a single-photon pulse; in other words, the single-photon pulse  $\xi(t)$  is used as the control input. As  $\xi$  is the pulse shape of the single photon, it is in the space  $L^2(\mathbb{R}, \mathbb{C})$  with additional constraint that is  $L^2$  norm  $\|\xi\| = 1$ . The physical interpretation of this constraint can be found in Section 2.2 in [98]. The state of the first DQD qubit evolves according to the master equation (8.1). As  $\rho_{\text{DQD}_1}$  in (8.1) is the reduced density matrix of the first DQD qubit, thus it is a  $2 \times 2$  Hermitian matrix. For the

cost function, we may use the Frobenius norm  $\|\rho_{\text{DQD}_1}(T) - |e_1\rangle\langle e_1|\|_{\text{F}}^2$ . That is, we desire to steer the state of the first DQD qubit as close as possible to  $|e_1\rangle$  at a given time instance  $T$ . Moreover, as discussed in [99], to get a sparse signal which is often desirable in experiments, we may also add an  $L^1$  term  $\beta|\xi|_1$  in the cost function. In summary, to fit into (4.1) in [99], we may choose the following cost function

$$\|\rho_{\text{DQD}_1}(T) - |e_1\rangle\langle e_1|\|_{\text{F}}^2 + \beta \int_0^T |\xi(t)|_1 dt.$$

As  $\xi(t)$  is the pulse shape of the single-photon state to be designed, quantum physics demands the  $L^2$  norm  $\|\xi\|_2 \triangleq \sqrt{\int_0^T |\xi(t)|^2 dt} = 1$ . Thus, in the above formulation of the optimal control problem, the to-be-designed pulse shape is in the set  $\mathcal{C} = \{\xi : \|\xi\|_2 = 1\}$ . Clearly, this constraint makes the admissible set of  $\xi$  non-convex. In order to use quantum optimal control methods as those in [99–101], we have to remove this constraint. One possible way is the following: Firstly, we ignore the constraint imposed by  $\mathcal{C}$  and solve the optimization problem by means of quantum optimal control methods such as those in [99–101]. Assume the obtained solution is  $\xi(t)$  over the time interval  $[0, T]$ . Then let  $\gamma = \|\xi\|_2$ . If  $\gamma = 1$ , it is perfect, nothing else is needed. Otherwise, define  $\eta(t) \triangleq \gamma\xi\left(\frac{t}{\gamma}\right)$  over the time interval  $[0, \gamma T]$ . Then  $\|\eta\| = 1$ , we use  $\eta$ , a scaled version of  $\xi$ , instead of  $\xi$  as the pulse shape to be designed. Clearly,  $\eta$  accomplishes the job at the terminal time  $\gamma T$ . Solving this optimal control problem may be another future research direction.

## References

- [1] A. I. Lvovsky, H. Hansen, T. Aichele, O. Benson, J. Mlynek, and S. Schiller, “Quantum state reconstruction of the single-photon Fock state,” *Physical Review Letters*, vol. 87, no. 5, p. 050402, 2001.
- [2] Z. Yuan, B. E. Kardynal, R. M. Stevenson, A. J. Shields, C. J. Lobo, K. Cooper, N. S. Beattie, D. A. Ritchie, and M. Pepper, “Electrically driven single-photon source,” *Science*, vol. 295, no. 5552, pp. 102–105, 2002.
- [3] J. McKeever, A. Boca, A. D. Boozer, R. Miller, J. R. Buck, A. Kuzmich, and H. J. Kimble, “Deterministic generation of single photons from one atom trapped in a cavity,” *Science*, vol. 303, no. 5666, pp. 1992–1994, 2004.
- [4] A. A. Houck, D. Schuster, J. Gambetta, J. Schreier, B. Johnson, J. Chow, L. Frunzio, J. Majer, M. Devoret, S. Girvin, *et al.*, “Generating single microwave photons in a circuit,” *Nature*, vol. 449, no. 7160, pp. 328–331, 2007.
- [5] J. L. O’Brien, A. Furusawa, and J. Vučković, “Photonic quantum technologies,” *Nature Photonics*, vol. 3, no. 12, pp. 687–695, 2009.



- [6] G. Buller and R. Collins, “Single-photon generation and detection,” *Measurement Science and Technology*, vol. 21, no. 1, p. 012002, 2009.
- [7] A. I. Lvovsky and M. G. Raymer, “Continuous-variable optical quantum-state tomography,” *Reviews of modern physics*, vol. 81, no. 1, p. 299, 2009.
- [8] C. Santori, D. Fattal, and Y. Yamamoto, *Single-photon devices and applications*. John Wiley & Sons, 2010.
- [9] S. Buckley, K. Rivoire, and J. Vučković, “Engineered quantum dot single-photon sources,” *Reports on Progress in Physics*, vol. 75, no. 12, p. 126503, 2012.
- [10] M. Pechal, L. Huthmacher, C. Eichler, S. Zeytinoğlu, A. Abdumalikov Jr, S. Berger, A. Wallraff, and S. Filipp, “Microwave-controlled generation of shaped single photons in circuit quantum electrodynamics,” *Physical Review X*, vol. 4, no. 4, p. 041010, 2014.
- [11] P. Lodahl, S. Mahmoodian, and S. Stobbe, “Interfacing single photons and single quantum dots with photonic nanostructures,” *Reviews of Modern Physics*, vol. 87, no. 2, p. 347, 2015.
- [12] A. Reiserer and G. Rempe, “Cavity-based quantum networks with single atoms and optical photons,” *Reviews of Modern Physics*, vol. 87, no. 4, p. 1379, 2015.
- [13] H. I. Nurdin, M. R. James, and N. Yamamoto, “Perfect single device absorber of arbitrary traveling single photon fields with a tunable coupling parameter: A QSDE approach,” in *2016 IEEE 55th Conference on Decision and Control (CDC)*, pp. 2513–2518, IEEE, 2016.
- [14] H. Ogawa, H. Ohdan, K. Miyata, M. Taguchi, K. Makino, H. Yonezawa, J.-i. Yoshikawa, and A. Furusawa, “Real-time quadrature measurement of a single-photon wave packet with continuous temporal-mode matching,” *Phys. Rev. Lett.*, vol. 116, p. 233602, Jun 2016.
- [15] Z. H. Peng, S. E. D. Graaf, J. S. Tsai, and O. V. Astafiev, “Tuneable on-demand single-photon source,” *Nature Communications*, vol. 7, no. 12588, 2016.
- [16] X. Gu, A. F. Kockum, A. Miranowicz, Y.-x. Liu, and F. Nori, “Microwave photonics with superconducting quantum circuits,” *Physics Reports*, vol. 718, pp. 1–102, 2017.
- [17] A. O. Davis, V. Thiel, M. Karpiński, and B. J. Smith, “Measuring the single-photon temporal-spectral wave function,” *Physical review letters*, vol. 121, no. 8, p. 083602, 2018.
- [18] H. Wang, J. Qin, X. Ding, M.-C. Chen, S. Chen, X. You, Y.-M. He, X. Jiang, L. You, Z. Wang, *et al.*, “Boson sampling with 20 input photons and a 60-mode interferometer in a  $10^{14}$ -dimensional Hilbert space,” *Physical review letters*, vol. 123, no. 25, p. 250503, 2019.

- [19] K. Takase, M. Okada, T. Serikawa, S. Takeda, J.-i. Yoshikawa, and A. Furusawa, “Complete temporal mode characterization of non-Gaussian states by a dual homodyne measurement,” *Physical Review A*, vol. 99, no. 3, p. 033832, 2019.
- [20] M. Stobińska, G. Alber, and G. Leuchs, “Perfect excitation of a matter qubit by a single photon in free space,” *EPL (Europhysics Letters)*, vol. 86, no. 1, p. 14007, 2009.
- [21] Y. Wang, J. Minář, L. Sheridan, and V. Scarani, “Efficient excitation of a two-level atom by a single photon in a propagating mode,” *Physical Review A*, vol. 83, no. 6, p. 063842, 2011.
- [22] Y. Pan, G. Zhang, and M. R. James, “Analysis and control of quantum finite-level systems driven by single-photon input states,” *Automatica*, vol. 69, pp. 18–23, 2016.
- [23] E. Rephaeli, J.-T. Shen, and S. Fan, “Full inversion of a two-level atom with a single-photon pulse in one-dimensional geometries,” *Physical Review A*, vol. 82, no. 3, p. 033804, 2010.
- [24] J. E. Gough, M. R. James, H. I. Nurdin, and J. Combes, “Quantum filtering for systems driven by fields in single-photon states or superposition of coherent states,” *Physical Review A*, vol. 86, no. 4, p. 043819, 2012.
- [25] B. Q. Baragiola, R. L. Cook, A. M. Brańczyk, and J. Combes, “N-photon wave packets interacting with an arbitrary quantum system,” *Physical Review A*, vol. 86, no. 1, p. 013811, 2012.
- [26] H. Song, G. Zhang, and Z. Xi, “Continuous-mode multiphoton filtering,” *SIAM Journal on Control and Optimization*, vol. 54, no. 3, pp. 1602–1632, 2016.
- [27] Z. Dong, G. Zhang, and N. H. Amini, “Quantum filtering for a two-level atom driven by two counter-propagating photons,” *Quantum Information Processing*, vol. 18, no. 5, p. 136, 2019.
- [28] Z. Dong, G. Zhang, and N. H. Amini, “On the response of a two-level system to two-photon inputs,” *SIAM Journal on Control and Optimization*, vol. 57, no. 5, pp. 3445–3470, 2019.
- [29] C. Gardiner and P. Zoller, *Quantum Noise*. Springer, 2004.
- [30] E. B. Davies, *Quantum Theory of Open Systems*. Academic Press London, 1976.
- [31] H. M. Wiseman and G. J. Milburn, *Quantum Measurement and Control*. Cambridge university press, 2009.

- [32] J. Gough and M. R. James, “The series product and its application to quantum feedforward and feedback networks,” *IEEE Transactions on Automatic Control*, vol. 54, no. 11, pp. 2530–2544, 2009.
- [33] G. Zhang and M. R. James, “Quantum feedback networks and control: a brief survey,” *Chinese Science Bulletin*, vol. 57, no. 18, pp. 2200–2214, 2012.
- [34] J. E. Gough and G. Zhang, “On realization theory of quantum linear systems,” *Automatica*, vol. 59, pp. 139–151, 2015.
- [35] J. Combes, J. Kerckhoff, and M. Sarovar, “The SLH framework for modeling quantum input-output networks,” *Advances in Physics: X*, vol. 2, no. 3, pp. 784–888, 2017.
- [36] J. Zhang, Y.-x. Liu, R.-B. Wu, K. Jacobs, and F. Nori, “Quantum feedback: theory, experiments, and applications,” *Physics Reports*, vol. 679, pp. 1–60, 2017.
- [37] H. I. Nurdin and N. Yamamoto, *Linear Dynamical Quantum Systems - Analysis, Synthesis, and Control*. Springer-Verlag Berlin, 2017.
- [38] G. Zhang, S. Grivopoulos, I. R. Petersen, and J. E. Gough, “The Kalman decomposition for linear quantum systems,” *IEEE Transactions on Automatic Control*, vol. 63, no. 2, pp. 331–346, 2018.
- [39] C. W. Gardiner and M. J. Collett, “Input and output in damped quantum systems: Quantum stochastic differential equations and the master equation,” *Physical Review A*, vol. 31, no. 6, p. 3761, 1985.
- [40] K. Blow, R. Loudon, S. J. Phoenix, and T. Shepherd, “Continuum fields in quantum optics,” *Physical Review A*, vol. 42, no. 7, p. 4102, 1990.
- [41] S. Fan, S. E. Kocabas, and J. T. Shen, “Input-output formalism for few-photon transport in one-dimensional nanophotonic waveguides coupled to a qubit,” *Physical Review A*, vol. 82, p. 063821, 2010.
- [42] K. A. Fischer, R. Trivedi, V. Ramasesh, I. Siddiqi, and J. Vučković, “Scattering into one-dimensional waveguides from a coherently-driven quantum-optical system,” *Quantum*, vol. 2, p. 69, 2018.
- [43] N. Tezak, A. Niederberger, D. S. Pavlichin, G. Sarma, and H. Mabuchi, “Specification of photonic circuits using quantum hardware description language,” *Philosophical Transactions of the Royal Society A: Mathematical, Physical and Engineering Sciences*, vol. 370, no. 1979, pp. 5270–5290, 2012.

- [44] Z. Qin, A. S. Prasad, T. Brannan, A. MacRae, A. Lezama, and A. Lvovsky, “Complete temporal characterization of a single photon,” *Light: Science & Applications*, vol. 4, no. 6, pp. e298–e298, 2015.
- [45] D. F. Walls and G. J. Milburn, *Quantum Optics*. Springer Science & Business Media, 2007.
- [46] R. Loudon, *The Quantum Theory of Light*. OUP Oxford, 2000.
- [47] N. Yamamoto and M. R. James, “Zero-dynamics principle for perfect quantum memory in linear networks,” *New Journal of Physics*, vol. 16, no. 7, p. 073032, 2014.
- [48] H.-A. Bachor and T. C. Ralph, *A Guide to Experiments in Quantum Optics*. Wiley, 2004.
- [49] A. I. Lvovsky, “Squeezed light,” *Photonics: Scientific Foundations, Technology and Applications*, vol. 1, pp. 121–163, 2015.
- [50] J. E. Gough and G. Zhang, “Generating nonclassical quantum input field states with modulating filters,” *EPJ Quantum Technology*, vol. 2, pp. 2–15, 2015.
- [51] Z. Dong, L. Cui, G. Zhang, and H. Fu, “Wigner spectrum and coherent feedback control of continuous-mode single-photon Fock states,” *Journal of Physics A: Mathematical and Theoretical*, vol. 49, no. 43, p. 435301, 2016.
- [52] U. Titulaer and R. Glauber, “Density operators for coherent fields,” *Physical Review*, vol. 145, no. 4, p. 1041, 1966.
- [53] M. G. Raymer and I. A. Walmsley, “Temporal modes in quantum optics: then and now,” *Physica Scripta*, vol. 95, no. 6, p. 064002, 2020.
- [54] G. J. Milburn, “Coherent control of single photon states,” *The European Physical Journal Special Topics*, vol. 159, pp. 113–117, Jun 2008.
- [55] S. Hassani, *Mathematical Physics: a Modern Introduction to its Foundations*. Springer Science & Business Media, 2013.
- [56] G. Zhang and M. R. James, “On the response of quantum linear systems to single photon input fields,” *IEEE Transactions on Automatic Control*, vol. 58, no. 5, pp. 1221–1235, 2013.
- [57] J. E. Gough, M. James, and H. Nurdin, “Squeezing components in linear quantum feedback networks,” *Physical Review A*, vol. 81, no. 2, p. 023804, 2010.

- [58] G. Zhang and M. R. James, “Direct and indirect couplings in coherent feedback control of linear quantum systems,” *IEEE Trans. Automat. Contr.*, vol. 56, pp. 1535–1550, 2011.
- [59] G. Zhang, I. R. Petersen, and J. Li, “Structural characterization of linear quantum systems with application to back-action evading measurement,” *IEEE Transactions on Automatic Control*, vol. 65, no. 7, pp. 3157–3163, 2020.
- [60] M. R. James, H. I. Nurdin, and I. R. Petersen, “ $H^\infty$  control of linear quantum stochastic systems,” *IEEE Transactions on Automatic Control*, vol. 53, no. 8, pp. 1787–1803, 2008.
- [61] H. I. Nurdin, M. R. James, and A. C. Doherty, “Network synthesis of linear dynamical quantum stochastic systems,” *SIAM Journal on Control and Optimization*, vol. 48, no. 4, pp. 2686–2718, 2009.
- [62] W. R. Le Page, *Complex Variables and the Laplace Transform for Engineers*. Courier Corporation, 1980.
- [63] G. Zhang, “Analysis of quantum linear systems’ response to multi-photon states,” *Automatica*, vol. 50, no. 2, pp. 442–451, 2014.
- [64] G. Zhang, “Dynamical analysis of quantum linear systems driven by multi-channel multi-photon states,” *Automatica*, vol. 83, pp. 186–198, 2017.
- [65] J. E. Gough, M. R. James, and H. I. Nurdin, “Quantum filtering for systems driven by fields in single photon states and superposition of coherent states using non-markovian embeddings,” *Quantum information processing*, vol. 12, no. 3, pp. 1469–1499, 2013.
- [66] B. Q. Baragiola and J. Combes, “Quantum trajectories for propagating Fock states,” *Physical Review A*, vol. 96, no. 2, p. 023819, 2017.
- [67] H. Song, K. B. Kuntz, and E. H. Huntington, “Limitations on the quantum non-Gaussian characteristic of Schrödinger kitten state generation,” *New Journal of Physics*, vol. 15, no. 2, p. 023042, 2013.
- [68] V. Belavkin, “Quantum filtering of markov signals with white quantum noise,” *Elektronika*, vol. 25, pp. 1445–1453, 1980.
- [69] V. P. Belavkin, “Nondemolition measurements, nonlinear filtering and dynamic programming of quantum stochastic processes,” in *Modeling and Control of Systems*, pp. 245–265, Springer, 1989.
- [70] M. B. Plenio and P. L. Knight, “The quantum-jump approach to dissipative dynamics in quantum optics,” *Rev. Mod. Phys.*, vol. 70, pp. 101–144, Jan 1998.

- [71] R. van Handel, J. Stockton, and H. Mabuchi, “Feedback control of quantum state reduction,” *IEEE Transactions on Automatic Control*, vol. 50, no. 6, pp. 768–780, 2005.
- [72] L. Bouten, R. van Handel, and M. R. James, “An introduction to quantum filtering,” *SIAM Journal on Control and Optimization*, vol. 46, no. 6, pp. 2199–2241, 2007.
- [73] A. Barchielli and M. Gregoratti, *Quantum Trajectories and Measurements in Continuous Time: The Diffusive Case*, vol. 782. Springer, 2009.
- [74] P. Rouchon and J. F. Ralph, “Efficient quantum filtering for quantum feedback control,” *Physical Review A*, vol. 91, no. 1, p. 012118, 2015.
- [75] A. Dabrowska, G. Sarbicki, and D. Chruściński, “Quantum trajectories for a system interacting with environment in a single-photon state: Counting and diffusive processes,” *Physical Review A*, vol. 96, no. 5, p. 053819, 2017.
- [76] J. E. Gough, “An introduction to quantum filtering,” *arXiv preprint arXiv:1804.09086*, 2018.
- [77] Q. Gao, G. Zhang, and I. R. Petersen, “An exponential quantum projection filter for open quantum systems,” *Automatica*, vol. 99, pp. 59–68, 2019.
- [78] Q. Gao, G. Zhang, and I. R. Petersen, “An improved quantum projection filter,” *Automatica*, vol. 112, p. 108716, 2020.
- [79] A. M. Dabrowska, “From a posteriori to a priori solutions for a two-level system interacting with a single-photon wavepacket,” *JOSA B*, vol. 37, no. 4, pp. 1240–1248, 2020.
- [80] Z. Dong, G. Zhang, and N. H. Amini, “Single-photon quantum filtering with multiple measurements,” *International Journal of Adaptive Control and Signal Processing*, vol. 32, no. 3, pp. 528–546, 2018.
- [81] A. Serafini, S. De Siena, F. Illuminati, and M. G. Paris, “Minimum decoherence cat-like states in Gaussian noisy channels,” *Journal of Optics B: Quantum and Semiclassical Optics*, vol. 6, no. 6, p. S591, 2004.
- [82] A. M. Brańczyk and T. Ralph, “Teleportation using squeezed single photons,” *Physical Review A*, vol. 78, no. 5, p. 052304, 2008.
- [83] J. S. Neergaard-Nielsen, Y. Eto, C.-W. Lee, H. Jeong, and M. Sasaki, “Quantum tele-amplification with a continuous-variable superposition state,” *Nature Photonics*, vol. 7, no. 6, pp. 439–443, 2013.

- [84] K. Gheri, K. Ellinger, T. Pellizzari, and P. Zoller, “Photon-wavepackets as flying quantum bits,” *Fortschr. Phys.*, vol. 46, pp. 401–415, 1998.
- [85] C. Fabre and N. Treps, “Modes and states in quantum optics,” *Reviews of Modern Physics*, vol. 92, no. 3, p. 035005, 2020.
- [86] H.-S. Zhong, H. Wang, Y.-H. Deng, M.-C. Chen, L.-C. Peng, Y.-H. Luo, J. Qin, D. Wu, X. Ding, Y. Hu, *et al.*, “Quantum computational advantage using photons,” *Science*, vol. 370, no. 6523, pp. 1460–1463, 2020.
- [87] W. Asavanant, K. Takase, K. Fukui, M. Endo, J.-i. Yoshikawa, and A. Furusawa, “Wavefunction engineering via conditional quantum teleportation with a non-gaussian entanglement resource,” *Physical Review A*, vol. 103, no. 4, p. 043701, 2021.
- [88] T. C. Ralph, A. Gilchrist, G. J. Milburn, W. J. Munro, and S. Glancy, “Quantum computation with optical coherent states,” *Physical Review A*, vol. 68, no. 4, p. 042319, 2003.
- [89] A. Ourjoumtsev, H. Jeong, R. Tualle-Brouri, and P. Grangier, “Generation of optical ‘Schrödinger cats’ from photon number states,” *Nature*, vol. 448, no. 7155, pp. 784–786, 2007.
- [90] T. Gerrits, S. Glancy, T. S. Clement, B. Calkins, A. E. Lita, A. J. Miller, A. L. Migdall, S. W. Nam, R. P. Mirin, and E. Knill, “Generation of optical coherent-state superpositions by number-resolved photon subtraction from the squeezed vacuum,” *Physical Review A*, vol. 82, no. 3, p. 031802, 2010.
- [91] K. Huang, H. Le Jeannic, J. Ruauudel, V. Verma, M. Shaw, F. Marsili, S. Nam, E. Wu, H. Zeng, Y.-C. Jeong, *et al.*, “Optical synthesis of large-amplitude squeezed coherent-state superpositions with minimal resources,” *Physical review letters*, vol. 115, no. 2, p. 023602, 2015.
- [92] J. Etesse, M. Bouillard, B. Kanseri, and R. Tualle-Brouri, “Experimental generation of squeezed cat states with an operation allowing iterative growth,” *Physical review letters*, vol. 114, no. 19, p. 193602, 2015.
- [93] D. V. Sychev, A. E. Ulanov, A. A. Pushkina, M. W. Richards, I. A. Fedorov, and A. I. Lvovsky, “Enlargement of optical Schrödinger’s cat states,” *Nature Photonics*, vol. 11, no. 6, p. 379, 2017.
- [94] C. Oh and H. Jeong, “Efficient amplification of superpositions of coherent states using input states with different parities,” *JOSA B*, vol. 35, no. 11, pp. 2933–2939, 2018.

- [95] M. Eaton, R. Nehra, and O. Pfister, “Non-Gaussian and Gottesman–Kitaev–Preskill state preparation by photon catalysis,” *New Journal of Physics*, vol. 21, no. 11, p. 113034, 2019.
- [96] E. V. Mikheev, A. S. Pugin, D. A. Kuts, S. A. Podoshvedov, and N. B. An, “Efficient production of large-size optical Schrödinger cat states,” *Scientific Reports*, vol. 9, no. 1, pp. 1–15, 2019.
- [97] K. Takase, J.-i. Yoshikawa, W. Asavanant, M. Endo, and A. Furusawa, “Generation of optical Schrödinger cat states by generalized photon subtraction,” *Physical Review A*, vol. 103, no. 1, p. 013710, 2021.
- [98] Z. Dong, W. Cui, and G. Zhang, “On the dynamics of a quantum coherent feedback network of cavity-mediated double quantum dot qubits,” *arXiv:2004.03870*, 2020.
- [99] T. Breitenbach and A. Borzi, “A sequential quadratic hamiltonian scheme for solving non-smooth quantum control problems with sparsity,” *Journal of Computational and Applied Mathematics*, vol. 369, p. 112583, 2020.
- [100] G. Ciaramella and A. Borzi, “Quantum optimal control problems with a sparsity cost functional,” *Numerical Functional Analysis and Optimization*, vol. 37, no. 8, pp. 938–965, 2016.
- [101] A. Borzi, G. Ciaramella, and M. Sprengel, *Formulation and Numerical Solution of Quantum Control Problems*. SIAM, 2017.